

Probability and fidelity of teleportation in a two-mode continuous variable cluster state via an insufficiently selective measurement

J.A. Mendoza-Fierro[†] and L.M Arévalo Aguilar[†]

[†]Facultad de Ciencias Físico Matemáticas, Benemérita Universidad Autónoma de Puebla, 18 Sur y Avenida San Claudio, Col. San Manuel, Puebla 72520, Mexico

Abstract

Continuous-variable projective measurements can not select individual measurement results as in the discrete case; instead, the possible outcomes are bounded by the selectivity interval of the measurement; then, it is said that continuous-variable measurement devices are insufficiently selective. By utilizing this concept we show that the probability and fidelity of teleportation in a two-mode cluster state can be handled by the localization of the selectivity interval of the measurement apparatus. Besides, we provide a mathematical expression describing the probability distribution of the measurement outcomes in the two-mode cluster, which is a fundamental solution of the heat equation. In addition, we show that the fidelity of teleportation in the two mode cluster is given by the quotient between the squared solution of a non-homogeneous heat equation and the solution of the conventional heat equation. Furthermore, we extend our approach to a configuration involving successive clusters with intermediate corrections between each teleportation step. To exemplify our proposal, we consider the specific case of a squeezed-coherent state as the quantum state under teleportation.

1 Introduction

Quantum computation (QC) [1] exploits quantum phenomena such as entanglement and the principle of superposition to perform calculations and algorithms that surpass classical computers significantly. The revolutionary results include optimization problems [2, 3], fast simulation of complex quantum systems [4, 5], and speed-up in integers factorization [6]; thus, QC promises to improve enormously all generation of incoming technologies which will lay the foundation of an unprecedented advancement in human understanding of the nature [7]. Therefore, it is imperative to increase research in all branches that drive advancements in QC.

Currently, multiple models [8] exist for the realization of universal QC [9]; this paper, however, deals with the building-block of continuous variable (CV) one-way QC [10, 11]. The stratagem of this scheme involves the implementation of unitaries and algorithms via local projective measurements on a multipartite highly entangled system known as a cluster state. Remarkably, this model allows skip the requirement of unitary evolution which drives to the reduction of the number of necessary quantum gates for the processing of quantum information, which is carried principally by both the preparation of the entangled state and the structure of the measurements [12]. Notably, one-way QC has been proven to be fault-tolerant [13–16], providing a robust basis for error mitigation; besides, one-way QC offers an inherently adaptive framework since diverse entanglement structures and distinct measurements schemes provide the capacity to carry out different quantum algorithms [17].

Alternative to the employment of qubits for cluster construction in QC, we have the option of the continuous-variable (CV) approach [18], which weaves the cluster using quantum states expanded in a continuous eigenbasis [19]. The cornerstone for using these multipartite systems in universal QC was proposed in [20] utilizing the adaptation of the one-qubit teleportation circuit [21, 22] to the CV regime through an optical insight. In this context, perfect teleportation only happens

in the ideal situation where the sources building the cluster have infinite squeezing; however, in the real aim, only finite squeezing can be implemented, driving unavoidably to a Gaussian noise affecting the propagation of the information through the cluster [20].

Then, some of the current challenges to implementing efficient large-scale QC with CV cluster states involves seeking ways to deal with Gaussian imperfections due to finite squeezing, and achieve a determined threshold of noise for efficient operation. In the actual context, there are proposals for sidestep or lessen the cumulative noise due to the finite squeezing; for example, schemes of error correction [23, 24] and surface code [25–33] (see also [34] and references therein), error decreasing models by using a weighted controlled- Z operation [35] and the cubic phase gate [35], and the research in the evaluation of errors coming from different entangling operations [36]. However, in the current literature there no exists yet a formalism—to the best of our knowledge—that address the handling of Gaussian noise through the measurement mechanism itself in one-way QC with CV cluster states; this fact is specially relevant since one-way QC relies principally on the measurement mechanism. A first step to this goal is given in Ref. [37] where is recognized that the Gaussian noise affecting the teleportation in a two-mode CV cluster state is strongly dependent on the measurement outcome; that is, there will be some measurement values for which the effect of Gaussian distortions will be more severe, will other maintain a higher fidelity of the propagated quantum information. Then, this fact establishes an interesting question: *It is possible to use the measurement as a means to select a range of outcomes that allows to handle the Gaussian noise affecting the propagation of information through a two-mode CV cluster?* This question holds significant importance, as it enables us to delve into a—to the best of our knowledge—not yet considered aspect in the theoretical treatment of CV measurements in relation with the teleportation process through a two-mode cluster.

The premise to establish a link between the measurement and the Gaussian noise affecting the teleportation process in a two-mode cluster ranges from the fact that projective CV measurements can not be infinitely selective [38, 39]; that is, it can not select isolated outputs as in the case of observables with discrete eigenspectrum. Instead, CV measurements necessarily carry a finite range measurement results which are probabilistically distributed and whose scope is in relation with the selectivity range of the measurement device [38]. Even further, the conception of a projective measurement in the CV regime can be misunderstood, yielding a wrong formulation of a continuous-valued projection operator as a simple external product such as $|x\rangle\langle x|$ for x valued continuously, as is done explicitly in Ref. [40] in the context of the teleportation through a two-mode cluster. Besides of the mathematical troubles of this formulation, it not explains the probabilistic nature of the outcomes coming from the measurement carried on the cluster, which is a fundamental part of the formalism of the quantum measurement postulate [41].

Then, in this work, we answer the previously formulated question, showing how an insufficiently selective (projective) CV measurement allows us to handle the quality (probability and fidelity) of teleportation in the model of a two-mode CV cluster state as is presented in [20]. Besides, we provide a mathematical expression for the probability distribution of the measurement outcomes in the cluster which is the solution of the heat equation. In addition, we employ the formalism of an insufficiently selective measurement in a scheme of linear sequential teleportations; particularly, we derive exact mathematical expressions giving both the probability and fidelity of teleportation. It must be noted that the concatenation of two-mode cluster states in a linear sequence has been considered in the original proposal for universal quantum computation [20], but also in Ref. [37] from the perspective of the Wigner function (see also Ref. [42]); these papers show that the teleportation down the linear cluster provides a resultant Gaussian noise dependent on both the measurement results and the Gaussian envelopes of each step of the sequence; as a difference of these works, our proposed configuration considers between each step of the sequence the set of intermediate corrections applied in the case of an ideal cluster which relies on infinite squeezing [40]. To clarify our proposal, we will appeal to a squeezed-coherent state as the quantum mode to be teleported through the cluster state. In addition, we show that in both the single and the recursive scheme, insufficiently selective measurements necessarily carry a probability of getting or not fruitful teleportation as is expected from the quantum measurement formalism [43].

Hence, the research of this paper provides a first path for engineering schemes of linear two-mode cluster states that allow the handling of the inherent Gaussian through the measurement mechanism itself. Through this paper, we use shot-noise units ($\hbar = 2$), and the structure is

organized as follows: In Sec. 2, we review the CV quantum gates building a two-mode cluster state; besides, we delve into the concept of an insufficiently selective measurement device. In Sec. 3, by considering the formalism of an insufficiently selective measurement, we board the noisy teleportation process in a two-mode CV cluster state; besides, we obtain the expressions governing both the probability and the fidelity of teleportation; moreover, we explain how an insufficiently selective measurement allows handling these two parameters in the cluster. For clarification, we board a squeezed-coherent state as the system to be teleported. In Sec. 4, we treat the situation of sequential teleportations through a linear chain of two-mode cluster states, where we board again the quality of teleportation of a squeezed-coherent state from the perspective of the insufficiently selective measurement. We close the article with the conclusions in Sec. 5.

2 Preliminaries

In this section we review the pertinent CV quantum gates building the architecture of teleportation within a two-mode CV cluster state as is presented in Ref. [20] (see also [40]). Here, we do not provide an extensive review of the properties of these gates; for more details, see [44].

2.1 Important Continuous-Variable quantum gates

To start, we emphasize that the scope concerned with the current work is the CV quantum states—also referred to as quantum modes, for short—which are described through a continuous superposition of the position or momentum eigenbasis; that is, $\int dq \psi(q) |q\rangle$ or $\int dp \psi(p) |p\rangle$, where the basis set $\{|q\rangle\}$ and $\{|p\rangle\}$ are termed as the computational and the conjugate basis respectively. These states are in a relationship through a Fourier transform, that is,

$$|q\rangle = \frac{1}{2\sqrt{\pi}} \int dp e^{-\frac{i}{2}qp} |p\rangle, \quad (2.1)$$

$$|p\rangle = \frac{1}{2\sqrt{\pi}} \int dq e^{\frac{i}{2}qp} |q\rangle. \quad (2.2)$$

Now, we recover the generalization of the Pauli $\hat{\sigma}_x$ and $\hat{\sigma}_z$ operators, that is, the Heisenberg-Weyl operators $\hat{X}(r)$ and $\hat{Z}(s)$, which are generators of translations in the phase space; they are defined as

$$\hat{X}(r) = e^{-ir\hat{p}/2}, \quad (2.3)$$

$$\hat{Z}(s) = e^{is\hat{q}/2}. \quad (2.4)$$

These operators belong to the Heisenberg-Weyl group; moreover, they act on the position and momentum quadrature eigenstates of Eqs. (2.1) and (2.2) according to

$$\hat{X}(r) |q\rangle = |q+r\rangle, \quad \hat{Z}(s) |q\rangle = e^{is\hat{q}/2} |q\rangle, \quad (2.5)$$

$$\hat{X}(r) |p\rangle = e^{-ir\hat{p}/2} |p\rangle, \quad \hat{Z}(s) |p\rangle = |p+s\rangle. \quad (2.6)$$

In the Heisenberg picture, these gates act on the quadrature operators according to

$$\hat{X}(r)^\dagger \hat{q} \hat{X}(r) = \hat{q} + r, \quad \hat{X}(r)^\dagger \hat{p} \hat{X}(r) = \hat{p}, \quad (2.7)$$

$$\hat{Z}(s)^\dagger \hat{p} \hat{Z}(s) = \hat{p} + s, \quad \hat{Z}(s)^\dagger \hat{q} \hat{Z}(s) = \hat{q}. \quad (2.8)$$

The $\hat{X}(r)$ and $\hat{Z}(s)$ gates are related by $\hat{X}(r)\hat{Z}(s) = e^{-irs/2}\hat{Z}(s)\hat{X}(r)$. Moreover, in terms of the displacement operator $\hat{D}(\alpha) = \exp(\alpha\hat{a}^\dagger - \alpha^*\hat{a})$, the $\hat{X}(r)$ and $\hat{Z}(s)$ operators are $\hat{X}(r) = \hat{D}(r/2)$ and $\hat{Z}(s) = \hat{D}(is/2)$ respectively; then, the $\hat{X}(r)$ operator gives displacements in the real axis of the phase space while the $\hat{Z}(s)$ operator brings translations on the imaginary axis. A possible implementation of the displacement operators with optical elements involves imping an optical mode with a strong bright-coherent state on a beam splitter with a small coefficient reflection [44].

On the other hand, we recover the Fourier transform gate, which is the generalization of the Hadamard gate for qubits; this is defined as

$$\hat{F} = \exp\left(\frac{i\pi}{4}\right) \exp\left(\frac{i\pi}{2}\hat{a}^\dagger\hat{a}\right) = \exp\left[\frac{i\pi}{8}(\hat{q}^2 + \hat{p}^2)\right]. \quad (2.9)$$

In the phase-space description the Fourier gate represents a $\pi/2$ rotation from one quadrature to another, that is,

$$\hat{F}^\dagger\hat{q}\hat{F} = -\hat{p}, \quad \hat{F}^\dagger\hat{p}\hat{F} = \hat{q}. \quad (2.10)$$

The effect of the Fourier gate on the quadrature eigenstates is

$$\hat{F}|q\rangle = |p\rangle, \quad \hat{F}^\dagger|q\rangle = |-p\rangle, \quad (2.11)$$

$$\hat{F}|p\rangle = |-q\rangle, \quad \hat{F}^\dagger|p\rangle = |q\rangle; \quad (2.12)$$

besides, it acts on the $\hat{X}(r)$ and $\hat{Z}(s)$ gates according to

$$\hat{F}^\dagger\hat{Z}(s)\hat{F} = \hat{X}(s), \quad \hat{F}\hat{X}(r)\hat{F}^\dagger = \hat{Z}(r). \quad (2.13)$$

The Fourier gate represent a simply phase shift of the corresponding mode up to an overall phase factor [44]; therefore, it can be optically implemented through a delay on the mode by a lossless material with linear refraction index.

On the other hand, we have the controlled operation \hat{C}_Z , which is the quantum gate responsible for weaving the entanglement between the modes of the cluster; it is defined as

$$\hat{C}_Z = e^{\frac{i}{2}\hat{q}_c \otimes \hat{q}_t}, \quad (2.14)$$

where the labels in the exponential stand for (control \otimes target). The \hat{C}_Z gate causes displacements in phase-space on the target mode by a quantity determined by the position eigenvalue of the control mode.

In the Heisenberg frame the \hat{C}_Z gate carries the following transformations

$$\hat{C}_Z^\dagger\hat{q}_c\hat{C}_Z = \hat{q}_c, \quad \hat{C}_Z^\dagger\hat{q}_t\hat{C}_Z = \hat{q}_t, \quad (2.15)$$

$$\hat{C}_Z^\dagger\hat{p}_c\hat{C}_Z = \hat{p}_c + \hat{q}_t, \quad \hat{C}_Z^\dagger\hat{p}_t\hat{C}_Z = \hat{p}_t + \hat{q}_c. \quad (2.16)$$

Then, from Eqs. (2.15) and (2.16), we can observe that the control (target) quadrature defining the \hat{C}_Z remain as constant in their dynamics while the corresponding conjugate quadrature is just displaced by the position quadrature of the target (control). This behavior is consistent with the type of quantum no demolition (QND) Hamiltonians [19, 45, 46] which have the form $\hat{H}_Z = -\mathcal{K}(\hat{q}_i \otimes \hat{q}_j)$ being \mathcal{K} a coupling constant which it can experimentally adjust to one without generality loss. Then, the \hat{C}_Z gate act just unitary entangling interaction [47]. The experimental implementation comes through several mechanisms. For instance, it can be done optically [48], through beam splitter and inline squeezers [49, 50], or with atomic ensembles [51]. It is worth noting that another QND entangling interaction for cluster state generation can be accomplished through a SUM gate [52].

2.2 Insufficiently selective measurement apparatus

In this section, we delve into the concept of an insufficiently selective measurement device as is explained in [38] (Chapter 3, Sec. E2b). This concept is helpful for the correct mathematical definition of projective quantum measurements in the context of continuous-variable quantum systems. The ideas reviewed will find application in the design and analysis of noise affecting the scheme of teleportation utilizing CV cluster states.

Let us suppose a measurement apparatus that provides binary outcomes such as “yes” or “no” (click or no click, 1 or 0, positive or negative, etc.). Let us assume that this apparatus can measure a physical quantity represented by an observable \hat{A} of an arbitrary quantum state $|\psi\rangle$. If the measurement result falls inside an interval Δ on the real axis, the apparatus registers the “yes” response. Conversely, if the measured value lies outside this interval, the recorded result is “no.”

Then, such apparatus detects measurement results within a selectivity range Δ ; in the following, this quantity will be termed as *the power of resolution* or *selectivity interval* of the measurement. On the other hand, if the measurement device detects individual outputs, that is, single eigenvalues of the observable \hat{A} , we have a *completely selective measurement apparatus*. Nevertheless, if Δ contains several eigenvalues of \hat{A} , the device lacks the resolution needed to distinguish each possible result; then, we say it is *insufficiently selective*. For observables with continuous eigenspectrum—like the position or momentum of a quantum particle—it is not possible to *have completely selective measurement devices giving precise measurement results* [38] [53]. It must be noted that this argument must remain valid for any width of Δ since it will always contain an infinite number of eigenvalues, whatever their length on the real axis. Then, measurement apparatuses of observables with continuous eigenspectrum are, ever, insufficiently selective [38].

Let us return to the description of the measurement apparatus as provided earlier; then, we will focus on projective measurements of an observable \hat{X} with a continuous eigenspectrum. Be $\mathcal{S}_{\Delta X}$ the subspace of eigenstates of \hat{X} whose eigenvalues fall in a determined interval ΔX —that is, those measurement results for which the measurement device responses “yes”—. Then, we have the projection operator $\hat{P}_{\Delta X}$, which projects the quantum state $|\psi\rangle$ on the subspace $\mathcal{S}_{\Delta X}$ around a central eigenvalue X_0 contained inside the selectivity interval ΔX of the measurement device; mathematically, this projection operator is defined as

$$\hat{P}_{\Delta X} = \int_{X_0 - \Delta X/2}^{X_0 + \Delta X/2} dX |X\rangle \langle X|, \quad (2.17)$$

where $|X\rangle$ represent a eigenstate of the observable \hat{X} ; that is, $\hat{X}|X\rangle = X|X\rangle$ with $X \in \Delta X$, and $|X\rangle \in \mathcal{S}_{\Delta X}$. Besides, since \hat{X} represent an observable, then $\{|X\rangle\}$ constitutes a basis set in the subspace $\mathcal{S}_{\Delta X}$. Hence, our projective measurement apparatus will respond “yes” for eigenstates—or superpositions of them—of $\hat{P}_{\Delta X}$ with the eigenvalue of 1 and “no” for eigenstates of $\hat{P}_{\Delta X}$ with eigenvalue 0. It is worth noting that this measurement mechanism is essentially equivalent to measuring an observable with a degenerate eigenspectrum since there exists an infinity of states in $\mathcal{S}_{\Delta X}$ for which the measurement device will give the response “yes”.

It is important to note that the definition of Eq. (2.17) satisfies the adequate mathematical conditions for a projection operator; that is, $(\hat{P}_{\Delta X})^2 = \hat{P}_{\Delta X}$ and $\hat{P}_{\Delta X}|X\rangle = |X\rangle \forall |X\rangle \in \mathcal{S}_{\Delta X}$ (we have $\hat{P}_{\Delta X}|X'\rangle = 0 \forall |X'\rangle \notin \mathcal{S}_{\Delta X}$) as a difference of take the single external product $|X\rangle \langle X|$ which does not full fill the previous requirements for projective measurements [39]. In other words, we cannot—before the measurement—select a single eigenstate $|X\rangle$ to which the measured system will collapse; there exist, instead, a respective set of states for which the measurement apparatus will say “yes” and “no”, each with an associate probability distribution; then, as is usual in quantum mechanics, we only have at our disposal such probabilities. Regarding our measurement apparatus, the probability of getting the “yes” answer is given by

$$\mathcal{P}_{\text{yes}} = \langle \psi | \hat{P}_{\Delta X} | \psi \rangle, \quad (2.18)$$

where evidently we have $\mathcal{P}_{\text{no}} = 1 - \mathcal{P}_{\text{yes}}$. On the other hand, the postulate of reduction of the (pure) quantum state for this measurement remains as *If for the measurement of an observable \hat{X} with continuous eigenspectrum, on an arbitrary state $|\psi\rangle$, we obtain the response “yes” from the measurement device, the state $|\psi'\rangle$ of the system immediately after the measurement is the normalized projection of $|\psi\rangle$ on the subspace $\mathcal{S}_{\Delta X}$, that is,*

$$|\psi'\rangle = \frac{\hat{P}_{\Delta X} |\psi\rangle}{\sqrt{\langle \psi | \hat{P}_{\Delta X} | \psi \rangle}}. \quad (2.19)$$

Restricting ourselves to the realm of light detection, many insufficiently selective measurement devices are prevailing. For instance, photomultiplier tube devices can select impinging light photons in a determined range of wavelength depending on a diversity of factors such as the photo-sensible surface, the operation mode, and the quantum efficiency of its photocathode [54]. Also, we have electron counting devices and all families of semiconductor diodes detecting light quanta, including avalanche, photo, and PIN diodes whose detection range is dependent on various factors; for example, the bandgap of the valence and conduction band of the considered semiconductor [55] and even the surface area of the device.

3 Teleportation with finite squeezing in a two-mode continuous-variable cluster state

3.1 Noisy Gaussian teleportation process

To elucidate the concept of Gaussian noise due to finite squeezing in CV cluster states, we consider the quantum circuit for the teleportation of a gate as outlined originally in Ref. [20]. In the ideal scenario of this scheme, we generate a continuous-variable cluster state through the entanglement of a zero-momentum eigenstate $|0\rangle_p$ with an arbitrary system $|\psi\rangle$ by utilizing a \hat{C}_Z gate; then, a single projective measurement is performed on the mode containing the arbitrary state; through this, we can recover—through unitary corrections—the state $|\psi\rangle$ from the output of the mode that was initially associated with the zero-momentum eigenstate; see Ref. [40] for a detailed explanation. Crucially, within this framework, one can execute an algorithm \hat{U} on the teleported state by simply performing measurements in the eigenbasis of the operator $\hat{U}^\dagger \hat{p} \hat{U}$, where \hat{U} is a quantum operator that is diagonal in the computational basis and, consequently, commutes with the C_Z gate. This process represents the basis for the measurement-based quantum computing model for continuous variables, allowing the concatenation of these kinds of circuits to build up a large-scale cluster state. However, in practice, there is no physical way to generate zero momentum eigenstates since they constitute a non-normalizable set, which would need infinite energy to create them. Then, in substitution, these states are approximated by squeezed vacuum states, which—due to the finite squeezing—inevitably introduce a Gaussian noise that affects the teleportation of the state [20]. In the following, we give a detailed analysis of this process by including the concept of an insufficiently selective measurement explained in Sec. 2.2.

We consider the circuit of Fig. 1. Our input consists of an arbitrary state $|\psi\rangle$ on line 1 (top wire) and a squeezed vacuum state $|0, V_s\rangle$ on line 2 (bottom wire). We expand both states in position space according to

$$|\psi\rangle = \int dq \psi(q) |q\rangle, \quad (3.1)$$

and

$$|0, V_s\rangle = \left(\frac{V_s^2}{2\pi}\right)^{\frac{1}{4}} \int dq e^{-V_s^2 q^2/4} |q\rangle, \quad (3.2)$$

where V_s^2 is a positive parameter related to the variances of the position and momentum probability distributions of the state according to $\delta_q^2 = 1/V_s^2$ and $\delta_p^2 = V_s^2$ respectively; then, we can verify the saturation of the Heisenberg uncertainty relation $\delta_q^2 \delta_p^2 = 1$; besides, if $\delta_{q_i}^2$ ($\delta_{p_i}^2$) < 1 , we have squeezing in the position (momentum) distribution. In an optical context, the primary method for the generation of the states of Eq. (3.2) is the degenerate regime of the spontaneous parametric down-conversion [56, 57]. The initial state entering the circuit is the product $|\psi\rangle |0, V_s\rangle$; then, by applying the C_Z gate, we obtain the entangled state characterizing the cluster as

$$\hat{C}_Z |\psi\rangle |0, V_s\rangle = \left(\frac{V_s^2}{2\pi}\right)^{\frac{1}{4}} \int dq_1 dq_2 \psi(q_1) e^{-V_s^2 q_2^2/4} e^{\frac{i}{2} q_1 q_2} |q_1\rangle |q_2\rangle. \quad (3.3)$$

The next step is to apply an insufficiently selective measurement on the first line of the cluster on the momentum basis; this is carried by the following projection operator

$$\hat{P}_\Delta = \hat{P}_{\Delta p_1} \otimes \mathbb{I}_2, \quad (3.4)$$

where \mathbb{I}_2 is the unity operator for the second mode and $\hat{P}_{\Delta p_1}$ is given by

$$\hat{P}_{\Delta p_1} = \int_{p'_1 - \Delta p_1/2}^{p'_1 + \Delta p_1/2} dp_1 |p_1\rangle \langle p_1|, \quad (3.5)$$

which corresponds to an adequate projector operator centred around p'_1 within a selectivity range Δp_1 (see Section 2.2). Then, applying \hat{P}_Δ to Eq. (3.3), and making use of $\langle p|q\rangle = (2\sqrt{\pi})^{-1} e^{-iqp/2}$,

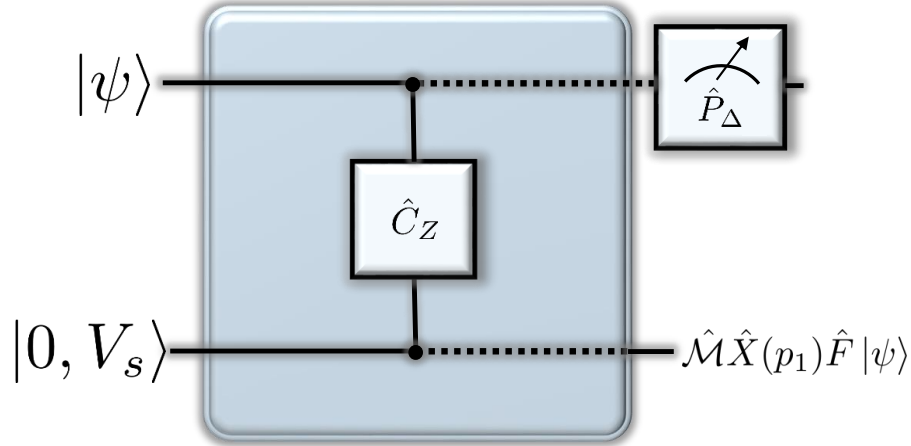


Figure 1: Quantum circuit for noisy Gaussian teleportation of an arbitrary state $|\psi\rangle$. The input states become entangled (dotted lines) through a \hat{C}_Z gate. Subsequently, we perform an insufficiently selective projective measurement on the first mode; then, for all possible outputs inside the selectivity region of the measurement, we get the state $\hat{\mathcal{M}}\hat{X}(p_1)\hat{F}|\psi\rangle$ in the second mode of the circuit.

we obtain

$$\hat{P}_\Delta\hat{C}_z|\psi\rangle|0, V_s\rangle = \left(\frac{V_s^2}{2\pi}\right)^{\frac{1}{4}} (2\sqrt{\pi})^{-1} \int_{p'_1-\Delta p_1/2}^{p'_1+\Delta p_1/2} dp_1 \int dq_1 dq_2 \psi(q_1) e^{-V_s^2 q_2^2/4} e^{\frac{i}{2}q_1 q_2} e^{-\frac{i}{2}p_1 q_1} |p_1\rangle |q_2\rangle, \quad (3.6)$$

which can be rewritten as

$$\hat{P}_\Delta\hat{C}_z|\psi\rangle|0, V_s\rangle = \int_{p'_1-\Delta p_1/2}^{p'_1+\Delta p_1/2} dp_1 |p_1\rangle \left(\hat{\mathcal{M}}\hat{X}(p_1)\hat{F}|\psi\rangle\right). \quad (3.7)$$

According to the postulate of quantum measurement for continuous variables of Eq. (2.19), the normalized state after measurement is the normalized projection—i.e., divided by the constant $N = (\mathcal{P}_{\text{tel}})^{1/2}$ —of Eq. (3.7) on the selectivity interval of the measurement. Then, this state implies that there will be successful teleportation for each of the momentum eigenstates of the first mode whose eigenvalues fall inside the selectivity interval of the measurement. It is worth noting that this mechanism corresponds to the measurement of an observable with a degenerate spectrum [38]; then, under this condition, the entanglement preserves on the selectivity region of the measurement (see, for example, Ref. [58] where measurements with degenerate spectrum can preserve entanglement); instead, a perfectly selective measurement unambiguously select one momentum eigenstate, which drives that the second mode of the cluster unequivocally collapses to the single state: $N^{-1}\hat{\mathcal{M}}\hat{X}(p_1)\hat{F}|\psi\rangle$, and the entanglement is destroyed.

After the measurement, some information regarding the teleported state lives on the second mode of the cluster, we obtain the corresponding state through the partial trace $\hat{\rho}_2 = \text{Tr}_1[\hat{\rho}_{12}]$, where $\hat{\rho}_{12} = \hat{P}_\Delta\hat{C}_z|\psi\rangle|0, V_s\rangle\langle V_s, 0|\langle\psi|\hat{C}_z^\dagger\hat{P}_\Delta^\dagger$ is the global density operator of the cluster; then, by utilizing Eq. (3.7), and choosing a basis $\{|p'_1\rangle\}$ inside Δp_1 to carry out the trace, the post-measurement normalized density operator associated with the second mode of the cluster is

$$\hat{\rho}_2 = N^{-2} \int_{p'_1-\Delta p_1/2}^{p'_1+\Delta p_1/2} dp_1 \hat{\mathcal{M}}\hat{X}(p_1)\hat{F}\hat{\rho}_{\text{in}}\hat{F}^\dagger\hat{X}^\dagger(p_1)\hat{\mathcal{M}}^\dagger, \quad (3.8)$$

where $\hat{\rho}_{\text{in}} = |\psi\rangle\langle\psi|$ is the density operator of the state under teleportation, and N is the normalization constant previously established; besides,

$$\hat{\mathcal{M}} = \int dq f_G(q) |q\rangle\langle q|, \quad (3.9)$$

is an operator which implies a Gaussian distortion; its effect can be visualized by calculating the wave function in the second mode of the cluster for each of the measurement outcomes inside the selectivity region Δp_1 ; that is, by taking the position basis $\{|q\rangle\}$, we calculate $\psi'(q) = \langle q | \hat{\mathcal{M}} \hat{X}(p_1) \hat{F} | \psi \rangle$, obtaining

$$\psi'(q) = \psi(q) f_G(q + p_1), \quad \forall p_1 \in \Delta p_1, \quad (3.10)$$

where the function $f_G(q)$ is given by

$$f_G(q) = \left(\frac{V_s^2}{2\pi} \right)^{\frac{1}{4}} e^{-V_s^2 q^2 / 4}, \quad (3.11)$$

and comes from the components $f_G(q) = \langle q | 0, V_s \rangle$ of the squeezed vacuum state of Eq. (3.3). Then, by considering an insufficiently selective measurement, the Eq. (3.8) means that the post-measurement state in the second mode of the cluster carries the information of the teleported state modulated by a Gaussian envelope displaced on a range Δp_1 whose center is p_1' .

On the other hand, the corresponding wave function in momentum space of Eq. (3.10) can be obtained through a Fourier transform; that is,

$$\begin{aligned} \psi(p) &= N^{-1} \mathcal{F} \{ \psi(q) f_G(q + p_1) \} \\ &= N^{-1} \mathcal{F} \{ \psi(q) \} * \mathcal{F} \{ f_G(q + p_1) \}, \quad \forall p_1 \in \Delta p_1, \end{aligned} \quad (3.12)$$

Therefore, $\psi(p)$ is given by the convolution between the wave functions in the momentum space of the teleported state and the squeezed vacuum state displaced by the measurement output.

On the other, as can be inferred from Eq. (3.7), there is an infinite of momentum values inside Δp_1 for which there will be successful teleportation through the cluster; the probability of this event is stipulated by the postulate of quantum measurement (see Eq. (2.18)); consequently, it follows that some measurement processes may yield teleportation while others may not. Notably, this probabilistic mechanism is not adequately captured by taking a projection operator given by the simple external product $|p\rangle \langle p|$ as is explicitly done in [40]. Then, in the following subsection, we utilize the concept of an insufficiently selective measurement to derive the mathematical expression giving the probability of teleportation in the context of a CV two-mode cluster.

3.2 Probability of teleportation

The Eq. (3.7) depicts the projection of the entangled state $\hat{C}_z |\psi\rangle |0, V_s\rangle$ onto the selectivity interval of the momentum measurement carried out on the first mode of the cluster; for each value of momentum contained in it, we will achieve noisy Gaussian teleportation of the state $|\psi\rangle$ to the second mode of the circuit. Per the postulate of the quantum measurement, the measurement apparatus sometimes will get teleportation, and other times not (see Eq. (2.18)); we cannot predict with certitude these events; instead, we only have the probabilities for each result. One experimentalist, of course, seeks to obtain the maximum probability for teleportation to guarantee the transmission of the information contained in the arbitrary state $|\psi\rangle$, but this fact depends on the experimental limitations concerning the selectivity interval of the measurement as well as the degree of squeezing used to build the cluster; we clarify these facts in the following.

The probability \mathcal{P}_{tel} for obtaining a result inside the selectivity region of the measurement for the cluster of Fig. 1 is given by Eq. (2.18); then, using Eq. (3.7), we have

$$\begin{aligned} \mathcal{P}_{\text{tel}} &= \langle \Psi | \hat{P}_\Delta | \Psi \rangle \\ &= \langle 0, V_s | \langle \psi | \hat{C}_z^\dagger \hat{P}_\Delta^\dagger \hat{P}_\Delta \hat{C}_z | \psi \rangle | 0, V_s \rangle \\ &= \int_{p_1' - \Delta p_1 / 2}^{p_1' + \Delta p_1 / 2} dp_1 P(p_1), \end{aligned} \quad (3.13)$$

where in the second line we use $|\Psi\rangle = \hat{C}_z |\psi\rangle |0, V_s\rangle$ and the properties of the projection operator $\hat{P}_\Delta^\dagger = \hat{P}_\Delta$ and $\hat{P}_\Delta^2 = \hat{P}_\Delta$; besides,

$$\begin{aligned} P(p_1) &= \langle \psi | \hat{F}^\dagger \hat{X}^\dagger(p_1) \hat{\mathcal{M}}^\dagger \hat{\mathcal{M}} \hat{X}(p_1) \hat{F} | \psi \rangle \\ &= \int dq [f_G(q)]^2 \rho(q - p_1) \end{aligned} \quad (3.14)$$

represents the probability distribution associated with the momentum measurement outputs in the first mode of the cluster; moreover, $\rho(q) = |\psi(q)|^2$ is the probability distribution of the teleported state in position space, and $f_G(q)$ is given by Eq. (3.11). Hence, $P(p_1)$ is determined from the convolution between the probability distributions of the squeezed vacuum state and that of the teleported state. Remarkably, by setting the variance $\delta_q^2 = 2t$ for some $t > 0$ and taking the explicit dependence of $f_G(q)$ on this parameter, we will have $[f_G(q, t)]^2 = k(q, t)$, where $k(q, t) = (4\pi t)^{-1/2} \exp[-q^2/4t]$ represents the kernel for the generalized Weierstrass transform, which constitutes the fundamental solution of the heat equation¹ [59]. Hence, the probability distribution of the measurement results in the cluster is given by the mirror image of the generalized Weierstrass transform of $\rho(q)$, which is simply a smoothed version of the position probability distribution of the teleported state.

On the other hand, Eq. (3.13) implies that the probability of teleportation in the cluster can be essentially manipulated by the degree of squeezing of the squeezed vacuum state. To visualize this point, consider that in the limit $t \rightarrow 0$ (that is, the increasing of the squeezing in position of the squeezed vacuum state), the kernel $k(q, t)$ represents a Dirac delta; consequently, the integral of Eq. (3.14) will approximate the mirror image of the position probability distribution of the teleported state; thus, the integral of Eq. (3.13) will determine the probability of teleportation; that is, if the set of possible measurement outcomes of the first mode live entirely on Δp_1 we will have $\mathcal{P}_{\text{tel}} = 1$; conversely, if the selectivity interval encompasses a fraction of the total spectrum of results, then $\mathcal{P}_{\text{tel}} < 1$. However, in real experimental scenarios, finite squeezing is the only available option; then, in this regime, the integral of Eq. (3.14) represents a smoothed version of $\rho(q)$, which implies $\mathcal{P}_{\text{tel}} < 1$ even in the situation where the measurement results live entirely on the finite selectivity interval of the measurement.

Remarkably, it is possible to improve the probability of teleportation in the situation where the measurement device can only detect a range of the measurement results; for this, we can center the selectivity interval of the measurement apparatus on the region of momentum outcomes for which the position probability distributions of the squeezed vacuum state and the system under teleportation have a higher overlap—i.e., where the convolution of Eq. (3.14) maximizes—; consequently, the integral of Eq. (3.13) will reach the maximum values for the interval Δp_1 .

3.3 Fidelity of teleportation

The objective of any teleportation process is to transmit the information of an unknown quantum system to a distant location without disturbance; however, achieving this in realistic terms is challenging due to degrading effects that affect the information propagation. A straightforward method to quantify the quality of a teleportation process is by assessing its fidelity \mathcal{F} ; for a single pure state, this measure is defined as [60]:

$$\mathcal{F} \equiv \langle \psi_{\text{in}} | \hat{\rho}_{\text{out}} | \psi_{\text{in}} \rangle, \quad (3.15)$$

which is bounded according to $0 \leq \mathcal{F} \leq 1$. The fidelity of teleportation of Eq. (3.15) offers a direct mechanism for assessing the impact of finite squeezing and measuring the efficiency of information propagation within the cluster. In Ref. [37] is shown that the effect of the Gaussian noise affecting the information propagation within the cluster is strongly dependent on the measurement results; that is, there will be some measurement outcomes for which the resulting distorted state will be closest to the original state, while others results in less information about it. This issue can negatively affect the general quality of teleportation, mainly due to those disperser measurement outputs. Nonetheless, in the light of insufficiently selective measurement, the measurement results are not unbounded. Then, from this point, we focus on showing how the selectivity interval of the measurement—i.e., a proper bounding of the measurement results—can be harnessed to handle the fidelity of teleportation within a two-mode cluster.

To start, we recall that the post-measurement density operator in the second mode of the cluster is given by Eq. (3.8); in the subsequent, we will utilize the quasi-selective approximation to derive

¹In fact, one can show through simple derivation that the integral of Eq. (3.14) is also a solution of the heat equation.

the fidelity of teleportation; that is, we consider the case where the integrands of Eqs. (3.8) and (3.13) are approximately constant on Δp_1 ; with this, the output density operator reduces to

$$\hat{\rho}_2 \approx [P(p_1)]^{-1} \hat{\mathcal{M}} \hat{X}(p_1) \hat{F} \hat{\rho}_{\text{in}} \hat{F}^\dagger \hat{X}^\dagger(p_1) \hat{\mathcal{M}}^\dagger, \quad \forall p_1 \in \Delta p_1, \quad (3.16)$$

where $P(p_1)$ is given by Eq. (3.14). To obtain the output density operator, we follow the ideal scenario with infinite squeezing (see section B1 of [40]). In this scheme, the state in the second mode of the cluster collapses to $|\psi'\rangle = \hat{X}(p_1) \hat{F} |\psi\rangle$; then, the teleportation process is complete until we apply the corrections: $\hat{F}^\dagger \hat{X}^\dagger(p_1)$ to $|\psi'\rangle$; hence, following this approach, we obtain the following output density operator

$$\hat{\rho}_{\text{out}} = \hat{F}^\dagger \hat{X}^\dagger(p_1) \hat{\rho}_2 \hat{X}(p_1) \hat{F}, \quad \forall p_1 \in \Delta p_1; \quad (3.17)$$

this state carries an uncorrectable noise induced by the Gaussian distortion operator $\hat{\mathcal{M}}$ of Eq. (3.9) which is not unitary; that is, we cannot take $\hat{\mathcal{M}}^\dagger \hat{\mathcal{M}} \neq \hat{\mathbb{1}}$. By substituting (3.17) in Eq. (3.15), we obtain the fidelity of teleportation as

$$\mathcal{F} = \frac{1}{P(p_1)} \left[\int dq f_G(q) \rho(q - p_1) \right]^2, \quad \forall p_1 \in \Delta p_1 \quad (3.18)$$

where $f_G(q)$ is the Gaussian function of Eq. (3.11), and $\rho(q) = |\psi(q)|^2$ is the position probability distribution of the state under teleportation. Referring the reader to Section 3.2, the Gaussian function $f_G(q)$ is related to the kernel of the generalized Weierstrass transform according to $f_G(q) = [k(q, t)]^{1/2}$. Then, instead of the usual heat equation, the integral in the numerator of Eq. (3.18) is a solution of the following non-homogeneous version:

$$\frac{\partial^2 u(p_1, t)}{\partial p_1^2} - \frac{\partial u(p_1, t)}{\partial t} = \left(\frac{q + p_1}{4t} \right) \frac{\partial u(p_1, t)}{\partial p_1}, \quad t > 0, \quad p_1 \in \Delta p_1, \quad (3.19)$$

with the Dirichlet boundary condition

$$u(p_1, 0) = f(-p_1). \quad (3.20)$$

Therefore, the fidelity of teleportation in a two-mode CV cluster is described by the quotient between the squared solution of the non-homogeneous heat equation of Eq. (3.19) and the solution of the conventional heat equation².

On the other hand, the fidelity of Eq. (3.18) refers to a single teleportation process; however, depending on the context, several teleportations may be necessary to extract the statistic of the quantum information processed by the cluster; then, in this situation, the average state teleported through the cluster is mixed [37]. Such a state is obtained by averaging the output density operator of Eq. (3.17) with the probability distribution associated with the measurement results—which, of course, lives on the selectivity interval of the measurement—that is,

$$\hat{\rho}_{\text{out}}^{\text{av}} = \int_{p_1' - \Delta p_1/2}^{p_1' + \Delta p_1/2} dp_1 P(p_1) \hat{\rho}_{\text{out}}, \quad (3.21)$$

where the superscript ‘av’ means ‘average’. By utilizing Eqs. (3.15) and (3.21), the averaged fidelity on multiple teleportation processes is

$$\mathcal{F}^{\text{av}} = \int_{p_1' - \Delta p_1/2}^{p_1' + \Delta p_1/2} dp_1 \left[\int dq f_G(q) \rho(q - p_1) \right]^2. \quad (3.22)$$

However, under the quasi-selective approach, the inner integrand of Eq. (3.22) is approximately constant; then, by considering this and making use of Eq. (3.18), we can express the average fidelity as

$$\mathcal{F}^{\text{av}} = P(p_1) \Delta p_1 \mathcal{F}; \quad (3.23)$$

²This argument even remains valid for any chosen measurement basis since any resulting diagonal operator can be absorbed in the probability distribution $\rho(q - p_1)$ of the teleported state.

then, the average fidelity becomes directly proportional to both the probability distribution of the momentum measurement outcomes and the fidelity of individual teleportations; since these quantities directly depend on the overlap between $f_G(q)$ and $\rho(q - p_1)$, it follows that the average fidelity also depends on this overlap.

In the subsequent section, we will show—through a specific instance—how the bounding of the measurement results due to an insufficiently selective measurement allows the handling of both the probability and the fidelity of individual teleportations.

3.4 Teleportation of a squeezed-coherent state

To get insight into the impact of an insufficiently selective measurement on both the probability and fidelity of teleportation through the cluster, our analysis centers on the realm of individual teleportations; then, we must evaluate the Eqs. (3.13) and (3.18) for a specific input state; for this, we consider a squeezed-coherent state $|\alpha, \xi\rangle$, which is the more general (pure) single-mode quantum state [40]. Such state is generated according to $|\alpha, \xi\rangle = \hat{D}(\alpha)\hat{S}(\xi)|0\rangle$, where $\hat{D}(\alpha) = \exp(\alpha\hat{a}^\dagger - \alpha^*\hat{a})$ and $\hat{S}(\xi) = \exp[-(\xi(\hat{a}^\dagger)^2 + \xi^*\hat{a}^2)]$ are the displacement and the one-mode squeezing operators respectively; besides, we have the complex amplitude $\alpha = (q_0 + ip_0)/2$ and $\xi = re^{i\theta}/2$, being q_0 and p_0 the center of coordinates of the state under teleportation in the phase space and r and θ the squeezing and rotation parameters for $r \in \mathbb{R}$ and $0 \leq \theta \leq 2\pi$.

The wave function of a squeezed-coherent state has been determined by several methodologies [61]; at this step, we recover it ($\hbar = 2$) in the position space, it is,

$$\begin{aligned} \psi_{\xi, \alpha}(q) = \langle q | \alpha, \xi \rangle &= \left(\frac{1}{2\pi} \right)^{\frac{1}{4}} \frac{\sqrt{\cosh r_1 - e^{-i\theta} \sinh r_1}}{\sqrt{|\cosh r_1 - e^{i\theta} \sinh r_1|} \sqrt{|\cosh r_1 - e^{-i\theta} \sinh r_1|}} e^{\frac{i}{2} p_0 (q - \frac{q_0}{2})} \\ &\times \exp \left[-\frac{1}{4} \frac{\cosh r_1 + e^{i\theta} \sinh r_1}{\cosh r_1 - e^{i\theta} \sinh r_1} (q - q_0)^2 \right], \end{aligned} \quad (3.24)$$

where $r_1 \in \mathbb{R}$ is its squeezing parameter. The variances of the quadratures of position and momentum of this state are

$$\delta_q^2(r_1, \theta) = \cosh 2r_1 - \cos \theta \sinh 2r_1, \quad (3.25)$$

$$\delta_p^2(r_1, \theta) = \cosh 2r_1 + \cos \theta \sinh 2r_1. \quad (3.26)$$

Now, it must be noted that for the calculations of both the probability and the fidelity of teleportation (see Eqs. (3.14) and (3.18)), we need the position probability distribution of the teleported state displaced by the measurement outcome p_1 ; then, we include such value together the central coordinate of position of the squeezed-coherent state in order to define an effective displacement $X_0 = q_0 + p_1$, with $X_0 \in \mathbb{R}$; hence, using the wave function of Eq. (3.24) and considering the Eq. (3.25), we have the following ‘measurement-displaced’ position probability distribution of the squeezed-coherent state

$$\rho(q - p_1) = |\psi_{\xi, \alpha}(q - X_0)|^2 = [2\pi\delta_q^2(r_1, \theta)]^{-1/2} e^{-\frac{(q - X_0)^2}{2\delta_q^2(r_1, \theta)}}. \quad (3.27)$$

In the following sections, we will utilize Eq. (3.27) to analyze the teleportation process of the squeezed-coherent state through the cluster.

3.4.1 Probability of teleportation

Let us calculate, in general, the probability distribution for the measurement results in the teleportation process of a squeezed-coherent state through the two-mode cluster. By considering both the Gaussian function of Eq. (3.11) and the probability distribution of Eq. (3.27) in Eq. (3.14), we obtain

$$P(p_1) = \left(\frac{\sigma^2}{2\pi} \right)^{\frac{1}{2}} e^{-\sigma^2 X_0^2 / 2} \quad (3.28)$$

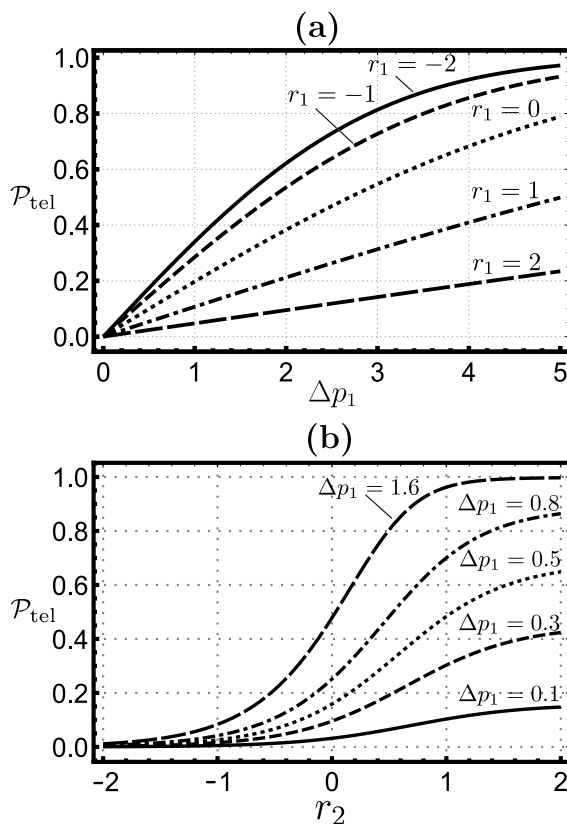


Figure 2: Probability of teleportation of the squeezed-coherent state versus (a) the width of the selectivity interval Δp_1 ($V_s^2 = 1, \theta = \pi$) for different squeezing parameters r_1 , and (b) the squeezing parameter of the squeezed vacuum state ($\delta_q^2(r_1, \theta) = 0.25, V_s^2 = e^{2r_2}$) for various widths of the selectivity interval. In these plots Δp_1 is centered on the central coordinate of the position of the squeezed-coherent state. Figures (a) and (b) show that the probability of teleportation increases when the selectivity interval of the measurement and the squeezing in position of both states building the cluster increases.

where $\sigma = \{V_s^2 / [1 + V_s^2 \delta_q^2(r_1, \theta)]\}^{1/2}$ and the dependence on p_1 is contained in the effective displacement X_0 . The Eq. (3.28)—and, in general, the Eq. (3.14)—besides representing the probability distribution of the momentum outcomes obtainable through the measurement in the first mode of the cluster, also provides a quantitative measure of the degree of overlap between the probability distributions of both the squeezed vacuum state and the state under teleportation; then, since the selectivity interval of the measurement is not unbounded, the probability to get teleportation is necessarily less than one; therefore, to guarantee the maximal probability of teleportation, we must center the selectivity interval on the point with maximal value for $P(p_1)$. For our particular instance, we have the peak at $X_0 = 0$; therefore, we need to center Δp_1 on the momentum value $p_1 = -q_0$, i.e., on the value of the position central coordinate of the coherent-squeezed state in phase space; then, following this central value, we integrate the probability distribution of Eq. (3.28) according to Eq. (3.13), the result is

$$\mathcal{P}_{\text{tel}} = \text{erf} \left(\frac{\Delta p_1 \sigma}{2\sqrt{2}} \right), \quad (3.29)$$

where $\text{erf}(x)$ is the error function. Since $\Delta p_1, \sigma > 0$, we will always have $\mathcal{P}_{\text{tel}} > 0$; then, as these two parameters increase, the probability of teleportation will also increase. The Eq. (3.29) implies that the likelihood of getting teleportation in the two-mode cluster is determined by both the width of the selectivity interval of the measurement and the squeezing properties of the states building the system. Notably, the increase of σ implies the increment of the parameter V_s^2 , which means a

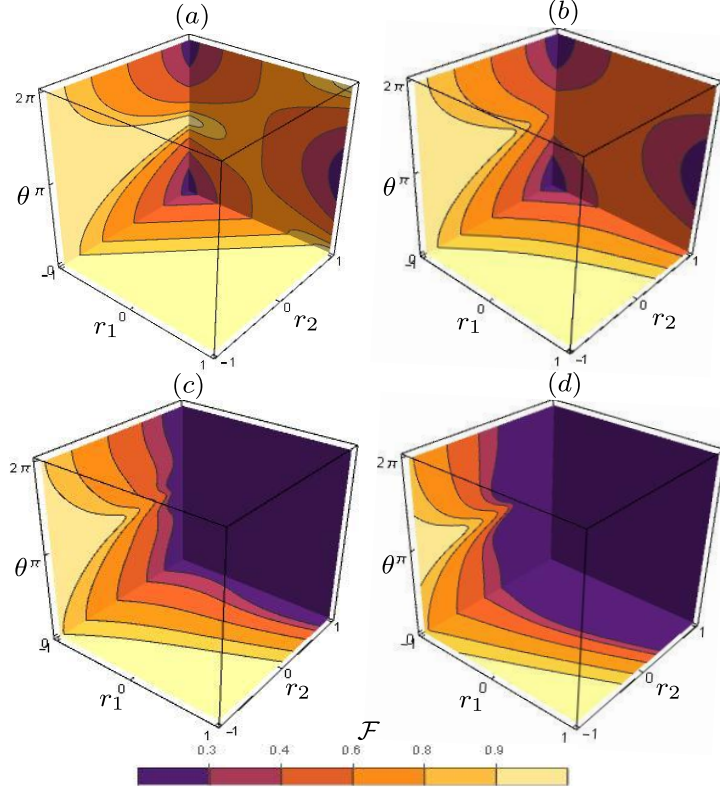


Figure 3: Behavior of the fidelity of teleportation \mathcal{F} of a squeezed-coherent state inside the three-dimensional region $\mathcal{R} = \{(r_1, r_2, \theta) \mid -1 \leq r_1 \leq 1, -1 \leq r_2 \leq 1, 0 \leq \theta \leq 2\pi\}$ for a two-mode cluster state with finite squeezing. The effective displacements are (a) $X_0 = 0$, (b) $X_0 = \pm 1$, (c) $X_0 = \pm 1.75$, (d) $X_0 = \pm 3.5$. The fidelity inside \mathcal{R} diminishes as the effective displacement increases.

higher squeezing in position for the squeezed vacuum state building the cluster. On the other hand, by considering the definition for σ , we conclude that the decreasing of the variance $\delta_q^2(r_1, \theta)$ of the squeezed-coherent state improves the probability of teleportation; the rotation angle optimizing such decreasing is $\theta = \pi$, for the region $r_1 < 0$.

In all the subsequent, we will utilize $V_s^2 = e^{2r_2}$ for the squeezed vacuum state, being $r_2 \in \mathbb{R}$ its squeezing parameter; therefore, such state will exhibit position (momentum) squeezing when $r_2 > 0$ ($r_2 < 0$); then, with these considerations, in Fig. 2, we plot the behavior for the probability of teleportation of the squeezed-coherent state versus (a) the width of the selectivity interval of the measurement and (b) the squeezing parameter of the squeezed vacuum state of the cluster.

3.4.2 Fidelity of teleportation

The fidelity of individual teleportations is given by Eq. (3.18); then, we use the function $f_G(q)$ of Eq. (3.11) and the probability distribution of Eq. (3.27) to evaluate the integral of such expression; through this process, we obtain the fidelity of teleportation for the squeezed-coherent state in the cluster as

$$\mathcal{F} = [P(p_1)]^{-1} \left(\frac{2}{\pi V_s^2} \right)^{\frac{1}{2}} \delta^2 e^{-(\delta X_0)^2}, \quad (3.30)$$

where $P(p_1)$ is the probability distribution for the momentum measurement outcomes, given by Eq. (3.28); besides, $\delta = \{V_s^2 / [2 + V_s^2 \delta_q^2(r_1, \theta)]\}^{1/2}$. In Fig. 3 we show \mathcal{F} inside the three-dimensional region

$$\mathcal{R} = \{(r_1, r_2, \theta) \mid -1 \leq r_1 \leq 1, -1 \leq r_2 \leq 1, 0 \leq \theta \leq 2\pi\} \quad (3.31)$$

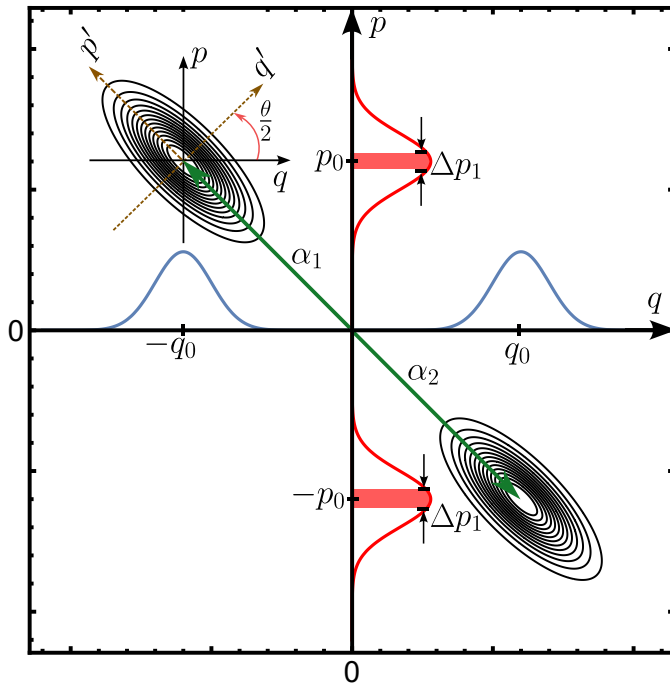


Figure 4: Instance to enhance the fidelity of teleportation of the squeezed-coherent state through a two-mode cluster. We prepare the squeezed-coherent state in the third or fourth quadrant of the phase space with centers $(-q_0, p_0)$ and $(q_0, -p_0)$ respectively, such that $|q_0| = |p_0|$; after building the cluster through the \hat{C}_z -gate, all the information of the momentum outcomes of the first mode is in the reduced density operator $\hat{\rho}_1$. Such a state has a Wigner function $W(q_1, p_1)$ (concentric ellipses) in phase space whose associated position (blue curves) and momentum (red curves) probability distributions are described by Gaussian centered in $\mp q_0$ and $\pm p_0$ respectively. The set of outputs that the insufficiently selective measurement apparatus can register is determined by the selectivity interval Δp_1 , which encompasses a portion of the domain of the momentum probability distribution associated with $\hat{\rho}_1$ (red filling under the red curve). Then, to get the maximal fidelity of teleportation, we must center the selectivity interval on $\pm p_0$ and adjust the width $|\Delta p_1|$ such that the possible measurement outputs are nearly closed to $\pm p_0$.

for different values of the magnitude of X_0 ; from that figure, it is evident that the fidelity shows a diminishing trend as the magnitude of X_0 increases. This observation is mathematically substantiated by considering the limit: $\lim_{X_0 \rightarrow \pm\infty} \mathcal{F} = 0$, which is an expected result since—as can be verified from Eq. (3.30)—the effective displacement comes into play through a Gaussian function centered in $X_0 = 0$, which attenuates the fidelity of teleportation as the magnitude of X_0 grows; this behavior indicates that the fidelity of teleportation for the squeezed-coherent state is influenced by the localization of the selectivity range of the measurement; therefore, we must center its localization on those measurement results for which the integral of Eq. (3.18) is maximum.

To illustrate the previous idea, we give a straightforward instance. Let us consider that the squeezed-coherent state we want to teleport is prepared in either the second or fourth quadrant of phase space with amplitudes $\alpha_1 = -q_0 + ip_0$ and $\alpha_2 = q_0 - ip_0$ respectively, such that $|q_0| = |p_0|$; hence, the central coordinates of this state are $(-q_0, p_0)$ and $(q_0, -p_0)$. Subsequently, we apply the \hat{C}_z gate to entangle this state with the squeezed vacuum state, getting with the state of Eq. (3.3); then, all possible momentum measurement results obtainable in the first mode are contained in the corresponding reduced density operator $\hat{\rho}_1 = \text{Tr}_2[\hat{\rho}_{12}]$, where $\hat{\rho}_{12} = \hat{P}_\Delta \hat{C}_z |\psi\rangle |0, V_s\rangle \langle V_s, 0| \langle \psi| \hat{C}_z^\dagger \hat{P}_\Delta^\dagger$ is the global density operator of the cluster. We can obtain the statistics of $\hat{\rho}_1$ through the Wigner quasi-probability distribution [62]; that is, by taking into account a position basis $\{|x\rangle\}$ for the first mode of the cluster, and the definition for the Wigner function (units of $\hbar = 2$) [63]: $W(q, p) = (4\pi)^{-1} \int du e^{iqu/2} \langle p + u/2 | \hat{\rho} | p - u/2 \rangle$, we obtain the

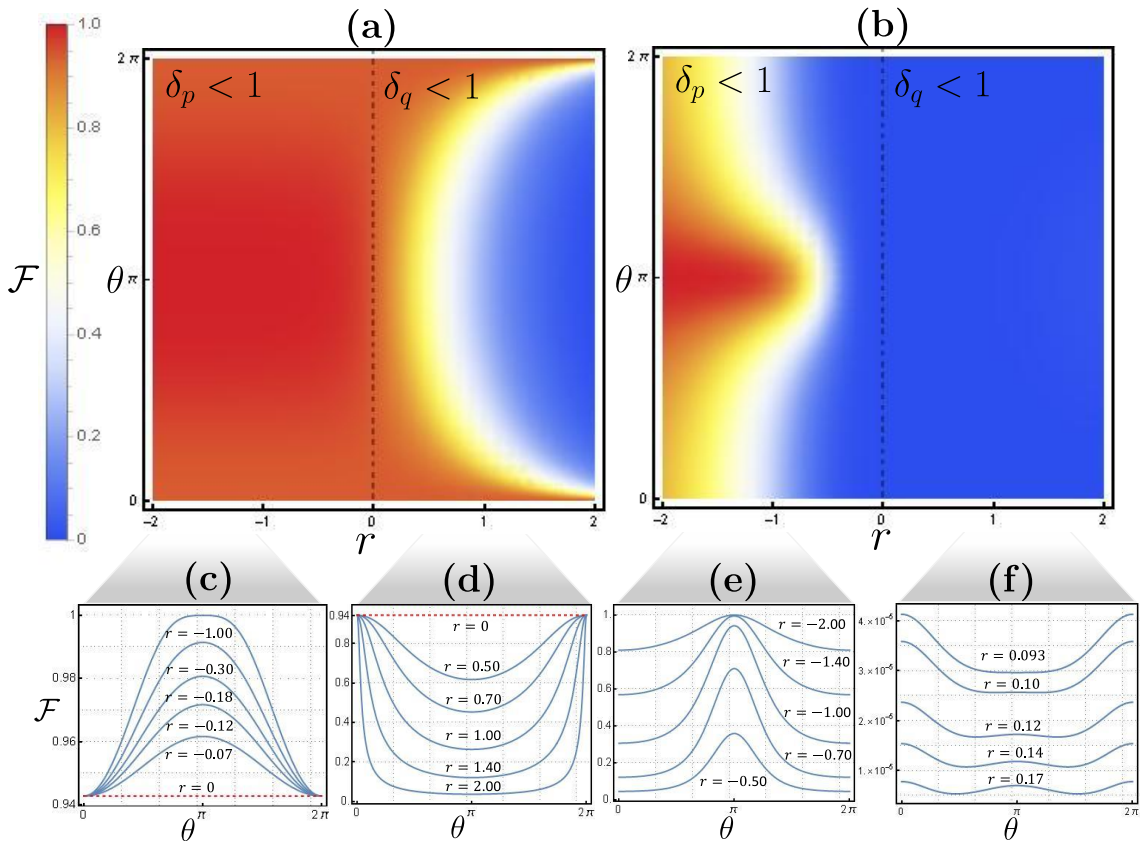


Figure 5: Density plots (figures (a) and (b)) and curves (figures (c) - (f)) for the fidelity of teleportation \mathcal{F} of a squeezed-coherent state through a two-mode cluster with finite squeezing. The squeezing parameters of the two states are $r_1 = r_2 = r$. The plots (a) and (b) describe the regimes of zero and non-zero effective displacements using $X_0 = 0$ and $X_0 = \pm 10$ respectively. Each plot is divided into the regions $r > 0$ and $r < 0$ by the dotted line of $r = 0$, pointing out the cases where the squeezed vacuum state of the cluster presents squeezing in the position and momentum probability distributions respectively; besides, this line represents the case where both states are coherent states. Figures (c)-(f) describe the behavior of the curves of fidelity as a function of the rotation angle θ for distinct r parameters inside the regions $r > 0$ and $r < 0$. Then, as the effective displacement increases, the region of low fidelity (blue colored) expands towards the region of $r < 0$, indicating that the squeezed vacuum state of the cluster requires progressively more squeezing in momentum to reach fidelities near to one.

joint probability distribution for position and momentum of the first mode of the cluster as

$$W(q_1, p_1) = \frac{1}{2\pi\hbar} \int dx du e^{iq_1 u/2} [f_G(x)]^2 \psi(x - p_1 - u/2) \psi^*(x - p_1 + u/2); \quad (3.32)$$

then, all possible measurement outputs are in the momentum probability distribution associated with the Wigner function of Eq. (3.32); that is, $P(p_1) = \int dq_1 W(q_1, p_1)$; therefore, we must center the selectivity interval Δp_1 on the momentum coordinate such that offers a greater overlap between the functions $f_G(q)$ and $\rho(q - p_1)$; for our specific instance, we must center it on p_0 ; see Fig. 4 for a sketch of this mechanism.

On the other hand, it is worth noting that the measurement results on the first mode of the cluster are—according to Eq. (3.13)—probabilistically distributed on the selectivity interval of the measurement; consequently, some outcomes may deviate further away from the central value p_0 , what implies greater values for the effective displacement X_0 and therefore, a lower fidelity of teleportation in some cases. Then, to enhance the fidelity of teleportation, we must take small enough Δp ; however, according to Eq. (3.13), this process necessarily carries the decrement in the

probability of teleportation; consequently, we can conclude that the likelihood and the fidelity of teleportation present a complementary relation regarding the width of the selectivity interval.

On the other hand, if the effective displacement X_0 is not near zero, we will need to increase the momentum squeezing of the squeezed vacuum state of the cluster to reach teleportation with high fidelity. This fact aligns with the concept of an ideal cluster wherein zero momentum eigenstates are utilized for achieving flawless teleportation [20]. To graphically visualize these arguments, we investigate the scenario where the squeezed-coherent state and the squeezed vacuum state building the cluster share identical squeezing parameters; that is, $r_1 = r_2 = r$. This election allows us to visualize the influence of the effective displacement in the fidelity of teleportation while maintaining some degree of generality. Then, in Fig. 5, we show the density plots for the fidelity of teleportation of the squeezed-coherent state for the cases of $X_0 = 0$ and $X_0 = \pm 10$. In both scenarios, the higher fidelities of teleportation happen when the squeezed vacuum state presents squeezing in momentum ($r < 0$); however, it must be noted that as the effective displacement increases, we will require greater squeezing in momentum to achieve high fidelity of teleportation.

Remarkably, in the regime of $X_0 = 0$, the cluster model consistently yields a fidelity of $2\sqrt{2}/3$ when both input modes are coherent states ($r = 0$) (the red dotted lines in (c) and (d) of Fig. 5); furthermore, this fidelity is also obtained when both the squeezed-coherent state and the squeezed vacuum state match in the squeezing orientation, that is for $\theta = 0$ and $\theta = 2\pi$. For our particular instance of the teleportation of a squeezed-coherent state, the higher fidelities happen at the regime of $X_0 \approx 0$; however, this not be necessarily true in the general case; that is, according to Eq. (3.18), the maximum fidelities will arise when the Gaussian wave function of the squeezed vacuum state has significant overlap with the displaced probability distribution of the teleported state; then, the experimentalist should take the more convenient preparation in phase space of the state to teleport to select those measurement results that allows enhancing the quality of teleportation in the cluster; thus, this mechanism is particularly important due for the possible experimental limitations surrounding the generation of a high degree of squeezing, where the peaks are actually around 15 Db [64].

4 Sequential teleportations

Quantum communication between two points of a large channel can be achieved more efficiently if the channel is divided into several segments [65]. This mechanism can lessen the degrading effects that affect the information propagation through realistic noisy channels; for instance, we can preserve the entanglement between the resources in each link of the chain, which results in a higher quality of transmitted information even despite the cumulative error due to the finite squeezing of the sources. In the following, we utilize an insufficiently selective measurement to analyze the scenario where n circuits like the one in Fig. 1 are concatenated together. The difference between our scheme and previous references [20, 37, 42] is that we consider between each step of the chain the corrections for successful teleportation employed in the ideal case of a cluster with infinite squeezing [40].

4.1 Probability of teleportation

The Eq. (3.13) shows that the probability of obtaining teleportation within the cluster of Fig. (1) is contingent upon three factors: (i) the selectivity interval of the insufficiently selective measurement, (ii) the degree of squeezing of the squeezed vacuum state of the cluster, and (iii) the convolution between the position probability distributions of the squeezed vacuum state and that of the teleported state. Notably, for a chain of n consecutive circuits like the one in Fig. 1, the input state in each cluster originates from the output of the previous one; consequently, all the prior factors have a direct impact on the probability of teleportation in the immediate subsequent cluster; in other words, the likelihood of teleportation in a determined cluster of the chain is dependent on the teleportation process in the previous clusters. To elucidate this, we calculate the likelihood of teleportation in the n th cluster of a lineal chain of sequential teleportations.

To start, we define the input state entering the $(n - 1)$ -th cluster; for this, we consider the quasi-selective approximation in each teleportation process (see subsection 3.3); besides, between

each link of the chain we implement the corrections $\hat{F}^\dagger \hat{X}^\dagger$ as we explain in subsection 3.3; with this considerations, the input state of each cluster is

$$|\psi_{\text{in}}\rangle = N^{-1} \hat{\mathcal{G}}_{(n-1)} \cdots \hat{\mathcal{G}}_{(0)} |\psi\rangle, \quad (4.1)$$

where the normalization constant is $N = \sqrt{\langle \psi | \hat{\mathcal{G}}_{(0)}^\dagger \cdots \hat{\mathcal{G}}_{(n-1)}^\dagger \hat{\mathcal{G}}_{(n-1)} \cdots \hat{\mathcal{G}}_{(0)} | \psi \rangle}$ ³. Besides, $\hat{\mathcal{G}}_{(i)} = \hat{F}^\dagger \hat{X}^\dagger \left(p_1^{(i)} \right) \hat{\mathcal{M}}_i \hat{X} \left(p_1^{(i)} \right) \hat{F}$ (for $i \neq 0$) is the operator that summarizes the set of continuous-variable quantum gates involved through the teleportation process inside the i -esim cluster; moreover, we define $\hat{\mathcal{G}}_{(0)} = \hat{\mathbb{1}}$, such that the state entering to the first cluster is the normalized state $|\psi\rangle$, just as is described in the formalism of the section 3.1. Furthermore, $p_1^{(i)}$ is the momentum outcome obtained after the measurement carried on the first mode of the i -th cluster; therefore, this value belongs to the selectivity interval $\Delta p_1^{(i)}$.

To establish the probability of teleportation, we must follow the same method of determining Eqs. (3.13) and (3.14); therefore, we need simply substituting in such equations the position probability distribution associated with the state of Eq. (4.1). By harnessing the unitarity of the Fourier gate and using a momentum basis $\{|-p\rangle\}$, we obtain by recurrence the position probability distribution associated with Eq. (4.1), it is

$$\varrho(q) = N^{-2} \prod_{i=0}^{n-1} \left[f_{G_{(i)}} \left(q + p_1^{(i)} \right) \right]^2 \rho(q), \quad (4.2)$$

with the normalization constant

$$N = \sqrt{\int dq \prod_{i=0}^{n-1} \left[f_{G_{(i)}} \left(q + p_1^{(i)} \right) \right]^2 \rho(q)}, \quad (4.3)$$

where $f_{G_{(i)}}(q)$ is the Gaussian wave function associated with the squeezed vacuum state of the i -esim cluster (see Eq. (3.11)), and $\rho(q)$ is the density of probability in position space of the quantum state entering to the chain; besides, we define $f_{G_{(0)}}(X) \equiv 1$, for $X \in \mathbb{R}$; therefore $\varrho(q) = \rho(q)$ for the case of one single cluster. It is worth noting that the position probability density of Eq. (4.2) includes a normalization constant as a difference of its equivalent of one single cluster; as is evident from Eq. (4.3), the behavior of such normalization constant depends on the overlap between the wave function summarizing the noise added by all previous the teleportation processes and that of the original state entering to the chain; then, as a consequence of this, we must expect a different behavior for the probability of teleportation in a sequence of clusters than the case of teleportation through a single one.

On the other hand, it is worth noting that the squared function $\left[f_G \left(q + p_1^{(i)} \right) \right]^2$ represents a Gaussian probability distribution function (PDF) centered around $p_1^{(i)}$. Notably, pairwise products of Gaussian PDFs result in another Gaussian PDF multiplied by a scale factor that has a Gaussian shape [66]; then, this fact can be used recursively for the product of \mathcal{N} Gaussian PDFs, which will give the general result of a Gaussian scale factor $S_{\mathcal{N}}$ multiplying a new Gaussian PDF $f_{G_{\mathcal{N}}} \left(q + \mathcal{P}_1^{(\mathcal{N})} \right)$ with variance $\delta_{q_{\mathcal{N}}}^2$ and center $\mathcal{P}_1^{(\mathcal{N})}$ [66]; that is,

$$\prod_{i=0}^{\mathcal{N}} \left[f_{G_{(i)}} \left(q + p_1^{(i)} \right) \right]^2 = S_{\mathcal{N}} \left[f_{G_{\mathcal{N}}} \left(q + \mathcal{P}_1^{(\mathcal{N})} \right) \right]^2, \quad (4.4)$$

where the resulting Gaussian:

$$f_{G_{\mathcal{N}}} \left(q + \mathcal{P}_1^{(\mathcal{N})} \right) = \left(\frac{1}{2\pi\delta_{q_{\mathcal{N}}}^2} \right)^{\frac{1}{4}} \exp \left[-\frac{\left(q + \mathcal{P}_1^{(\mathcal{N})} \right)^2}{4\delta_{q_{\mathcal{N}}}^2} \right] \quad (4.5)$$

³It can be verified that this normalization constant is equivalent to taking the normalization of each output state in the second line of each of the $n - 1$ clusters.

has variance and center respectively according to

$$\delta_{q_{\mathcal{N}}}^2 = \left(\sum_{i=1}^{\mathcal{N}} \frac{1}{\delta_{q_i}^2} \right)^{-1}, \quad (4.6)$$

$$\mathcal{P}_1^{(\mathcal{N})} = \left(\sum_{i=1}^{\mathcal{N}} \frac{p_1^{(i)}}{\delta_{q_i}^2} \right) \delta_{q_{\mathcal{N}}}^2; \quad (4.7)$$

besides, the scale factor $S_{\mathcal{N}}$ of Eq. (4.4) is given by

$$S_{\mathcal{N}} = \frac{1}{(2\pi)^{(\mathcal{N}-1)/2}} \sqrt{\frac{\delta_{q_{\mathcal{N}}}^2}{\prod_{i=1}^{\mathcal{N}} \delta_{q_i}^2}} \exp \left\{ -\frac{1}{2} \left[\sum_{i=1}^{\mathcal{N}} \frac{(p_1^{(i)})^2}{\delta_{q_i}^2} - \frac{(\mathcal{P}_1^{(\mathcal{N})})^2}{\delta_{q_{\mathcal{N}}}^2} \right] \right\}. \quad (4.8)$$

The terms $\delta_{q_i}^2$ and $p_1^{(i)}$ in Eqs. (4.6) to (4.8) represent respectively the variance of the position probability distribution of the squeezed vacuum state and the momentum measurement outcome both associated with the i -th cluster; these quantities contribute to the resulting Gaussian PDF of Eq. (4.5) as well as the Gaussian scale factor of Eq. (4.8); consequently, the probability for obtaining teleportation inside a determined cluster of the chain, is influenced by both the squeezing of each squeezed vacuum state and the measurement outcomes—i.e., each of the previous selectivity intervals—in the previous clusters; thus, according to this mechanism, we can conclude that the probability of teleportation through a chain of consecutive clusters is an example of conditional probability [67].

By utilizing Eqs. (4.4) to (4.8) in Eqs. (4.2) and (4.3), the position probability distribution simplifies to

$$\varrho(q) = N^{-2} \left[f_{G_{(n-1)}} \left(q + \mathcal{P}_1^{(n-1)} \right) \right]^2 \rho(q), \quad (4.9)$$

where

$$N = \sqrt{\int dq \left[f_{G_{(n-1)}} \left(q + \mathcal{P}_1^{(n-1)} \right) \right]^2 \rho(q)}; \quad (4.10)$$

hence, the probability of teleportation in the n th cluster of the chain is obtained by replacing $\rho(q) \rightarrow \varrho(q)$ in Eqs. (3.13) and (3.14).

4.2 Fidelity of teleportation

To determine the fidelity of teleportation of an arbitrary state $|\psi\rangle$ in the n th cluster of the chain, we follow the procedure outlined in Subsection 3.3. We construct the density operator associated with the output (normalized) state of the second mode of the n th cluster; for this, we utilize the state of the Eq. (4.1) and take the change $(n-1) \rightarrow n$ to construct the output density operator $\hat{\rho}_{\text{out}} = N^{-2} \left(\hat{\mathcal{G}}_{(n)} \cdots \hat{\mathcal{G}}_{(0)} \right) |\psi\rangle \langle\psi| \left(\hat{\mathcal{G}}_{(0)} \cdots \hat{\mathcal{G}}_{(n)} \right)^\dagger$; then, by employing Eq. (3.15) and leveraging the unitarity of the Fourier gate in the products $\left(\hat{\mathcal{G}}_{(n)} \cdots \hat{\mathcal{G}}_{(0)} \right)$, we obtain the fidelity for sequential teleportations as $\mathcal{F}_{\text{seq}} = N^{-2} \left[\langle\psi| \hat{F}^\dagger \left(\prod_{i=1}^n \hat{D}_i \right) \hat{F} |\psi\rangle \right]^2$ being $\hat{D}_i = \left[\hat{X}^\dagger \left(p_1^{(i)} \right) \hat{\mathcal{M}}_i \hat{X} \left(p_1^{(i)} \right) \right]$, and N the constant of normalization; besides, the subscript ‘seq’ stands for ‘sequential’, labelling the fidelity for sequential teleportations. By taking into account that $\hat{F} |\psi\rangle = \int dp \psi(p) |p\rangle$ and the definitions for $\hat{\mathcal{M}}_i$ and $\hat{X} \left(p_1^{(i)} \right)$, we obtain by recurrence the fidelity for sequential teleportations; it is

$$\mathcal{F}_{\text{seq}} = N^{-2} \left(\int dq \prod_{i=1}^n f_{G_{(i)}} \left(q + p_1^{(i)} \right) \rho(q) \right)^2, \quad (4.11)$$

where the normalization constant is

$$N = \left(\int dq \prod_{i=1}^n \left[f_{G_{(i)}} \left(q + p_1^{(i)} \right) \right]^2 \rho(q) \right)^{\frac{1}{2}}; \quad (4.12)$$

besides, $f_{G_{(i)}}(q)$ represents the Gaussian wave function associated with the i -th squeezed vacuum state, and $p_1^{(i)}$ is the momentum measurement outcome obtained in the i -th cluster; besides, $\rho(q) = |\psi(q)|^2$ represents the position probability distribution of the teleported state.

The Eqs (4.11) and (4.12) can be simplified by using the product of Gaussians of Eq. (4.4); besides, by considering Eq. (4.8) in Eqs. (4.11) and (4.12), we obtain that the quotient between the set of scale factors implied by Eq. (4.11) cancels; then, with these considerations, the fidelity of teleportation of Eq. (4.11) reduces to

$$\mathcal{F}_{\text{seq}} = (N)^{-2} \left[\int dq f_{G_{(n)}}(q + \mathcal{P}_1^{(n)}) \rho(q) \right]^2, \quad (4.13)$$

with

$$N = \left(\int dq \left[f_{G_{(n)}}(q + \mathcal{P}_1^{(n)}) \right]^2 \rho(q) \right)^{\frac{1}{2}}, \quad (4.14)$$

being $f_{G_{(n)}}(q + \mathcal{P}_1^{(\mathcal{N})})$ the resulting Gaussian of Eq. (4.5) ($n = \mathcal{N}$) which has center $\mathcal{P}_1^{(\mathcal{N})}$ and variance $\delta_{q_{\mathcal{N}}}^2$ of Eqs. (4.6) and (4.7) respectively.

By considering the change of variable $q' = q + \mathcal{P}_1^{(n)}$ in Eq. (4.13), we can conclude that the fidelity of teleportation through a series of n concatenated clusters is equivalent to the fidelity of teleportation through a single cluster (see Eq. (3.18)) whose squeezed vacuum state has associated a Gaussian wave function $f_{G_{(n)}}(q + \mathcal{P}_1^{(n)})$ in the position space. This result suggests that all components within the chain—namely, the sources generating the n squeezed vacuum states and the \hat{C}_z gates—can be consolidated into a unified configuration comprising a single squeezed vacuum source and a single \hat{C}_z gate. This finding aligns with the results of Ref. [42], where is demonstrated that a linear sequence of CV cluster states is equivalent to one single squeezing source and one single quantum non-demolition gate. Then given our result, all conclusions regarding the fidelity of teleportation through a single cluster remain valid (see Sec. (3.4.2)). Specifically, the fidelity of Eq. (4.13) is still a quotient between the squared solution of the non-homogeneous heat equation of Eq. (3.19) and the solution of the conventional heat equation; besides, the average fidelity of the chain also will be proportional to the fidelity of the individual teleportations (see Eq. (3.23)).

On the other hand, one must expect that as the number of clusters in the chain increases, the fidelity reduces due to the accumulated Gaussian noise from all teleportation processes; of course, we can lessen the effect of this noise by increasing the squeezing of each squeezed vacuum state of the chain, but in addition—as we explain in Subsec. 3.4—we can resort to the selectivity intervals of the measurements to select those outputs that provide a higher overlap between $f_{G_n}(q + \mathcal{P}_1^{(n)})$ and $\rho(q)$ —i.e., that furnish a greater fidelity of teleportation—In the following section, we will harness this idea to show the handling of both the probability and the fidelity of teleportation in the scheme of sequential clusters by considering again the instance of a squeezed-coherent state as the quantum state under teleportation.

4.3 Teleportation of a squeezed-coherent state through successive clusters

4.3.1 Probability of teleportation

To see the effect of sequential teleportations on the probability of teleportation, we examine a particular instance for the teleportation of the squeezed-coherent state of Eq. (3.24) in the n th cluster of the chain. We assume a configuration where each squeezed vacuum state of the sequence has the same wave function: $f_{G_{(i)}}(q) = f_G(q)$ of Eq. (3.11), with a variance $\delta_q^2 = e^{-2r_2}$; besides, we consider the case where the squeezed-coherent state under teleportation has the same squeezing that all squeezed vacuum states of the sequence (i.e., we take $\theta = 0$ and $r_1 = r_2 = r$ in Eqs. (3.25) and (3.26)). Moreover, we assume that each of the $(n - 1)$ selectivity intervals are centred on the central coordinate of position of the squeezed-coherent state under teleportation; hence, under the quasi-selective approximation each measurement result will have

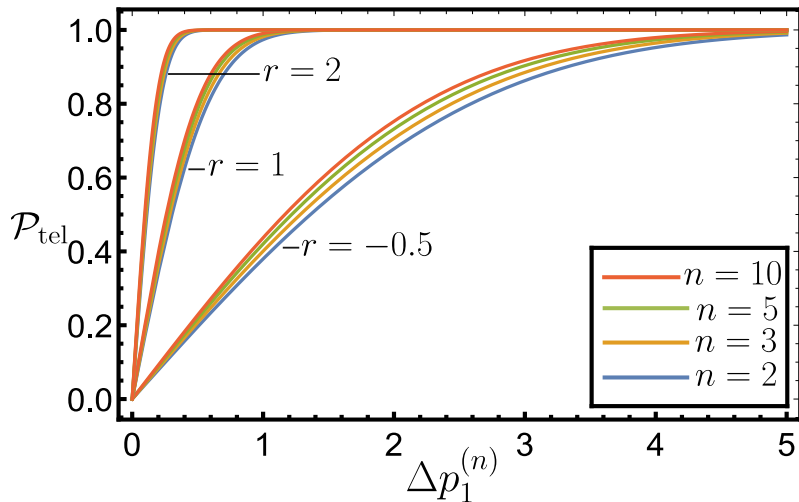


Figure 6: Plots for the probability of teleportation of the squeezed-coherent state through a chain of $n = 2, 3, 5,$ and 10 clusters ($\delta_{q_i}^2 = e^{-2r}$, $\theta = 0$, and $r_1 = r_2 = r$; therefore, $\delta_q^2(r_1, \theta) = \delta_{q_i}^2$) versus the width of the selectivity interval of the n th cluster.

$p_1^{(i)} \approx q_0$, being q_0 the central coordinate of the state of Eq. (3.24). With the last assumptions, the parameters of Eqs. (4.6) and (4.7) reduce to

$$\delta_{q_{\mathcal{N}}}^2 = (\mathcal{N}e^{2r_2})^{-1}, \quad (\mathcal{N} \geq 1), \quad (4.15)$$

$$\mathcal{P}_1^{(\mathcal{N})} = q_0. \quad (4.16)$$

Now, we use Eqs. (4.15) and (4.16) in the resultant Gaussian of Eqs. (4.9) and (4.10); then, we take the replace rule $\rho(q) \rightarrow \varrho(q)$ in Eq. (3.14); moreover, we use the initial probability density of Eq. (3.27), where this time the displacement will be the measurement outcome in the n th cluster; that is, $p_1^{(n)}$. It is important to clarify that we are not using the definition of some effective displacement; however, we need to center the selectivity interval of the n th cluster of the chain such that the possible measurement results offer the maximum probability of teleportation. Then, with these considerations we display in Fig. 6 the probability of teleportation of our particular scheme for $n = 2, 3, 5, 10$; for these cases, we carry out a numerical evaluation to find the optimal central value of the selectivity interval of the n th cluster; we find $p_1^{(n)} = 0, 1/3, 3/5,$ and $4/5$ respectively.

From Fig. 6, we deduce that the probability of obtaining teleportation through the sequence increases with the increasing of the squeezing in position of all states and the width of the selectivity interval of the n th cluster; this behavior is consistent with that of the teleportation process through a single cluster (see Section (3.4.1)). On the other hand, we have a higher probability of teleportation as the number of clusters of the chain is increasing; then, since the probability and fidelity of teleportation present a complementary behavior (see Subsection 3.4.2), we would expect that the fidelity of teleportation decreases with a larger chain of clusters as well as the decreasing of the squeezing in momentum of the squeezed vacuum states of the chain; we will very this fact in the following subsection.

4.3.2 Fidelity of teleportation

To obtain the fidelity of teleportation of the squeezed-coherent state in successive clusters, it must be noted that the expression of Eq. (4.13) for the fidelity of teleportation through the chain maintains the same mathematical shape as in the case for a single cluster (see Eq. (3.18) and consider the change of variable $q' = q + \mathcal{P}_1^{(n)}$ in Eqs. (4.13) and (4.14)); consequently, the fidelity of teleportation for a squeezed-coherent state through n consecutive clusters is obtained simply by taking the replace rule: $\delta_q^2 \rightarrow \delta_{q_{\mathcal{N}}}^2$ in Eqs. (3.30) and (3.28), where $\delta_{q_{\mathcal{N}}}^2$ is the variance of Eq. (4.6) and this time the effective displacement is defined in terms of the net displacement of the Eq. (4.7), that is $X_0 = q_0 + \mathcal{P}_1^{(\mathcal{N})}$.

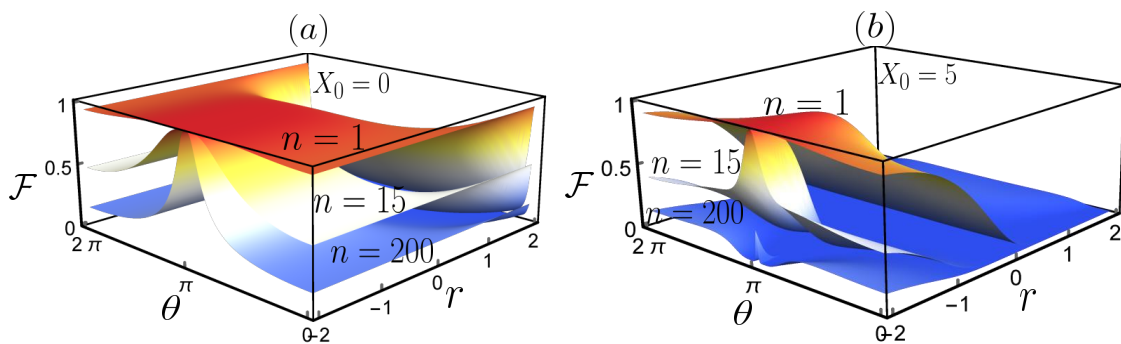


Figure 7: Effect of attenuation in the fidelity of teleportation of a squeezed-coherent state through n sequential clusters ($n = 1$, $n = 15$, and $n = 200$) for the cases of effective displacements of (a) $X_0 = 0$ and (b) $X_0 = 5$. As the state is teleported through a greater number of clusters, the fidelity decreases as a consequence of the Gaussian distortions induced in each step of the chain. The highest fidelities happen at the regime of zero effective displacement.

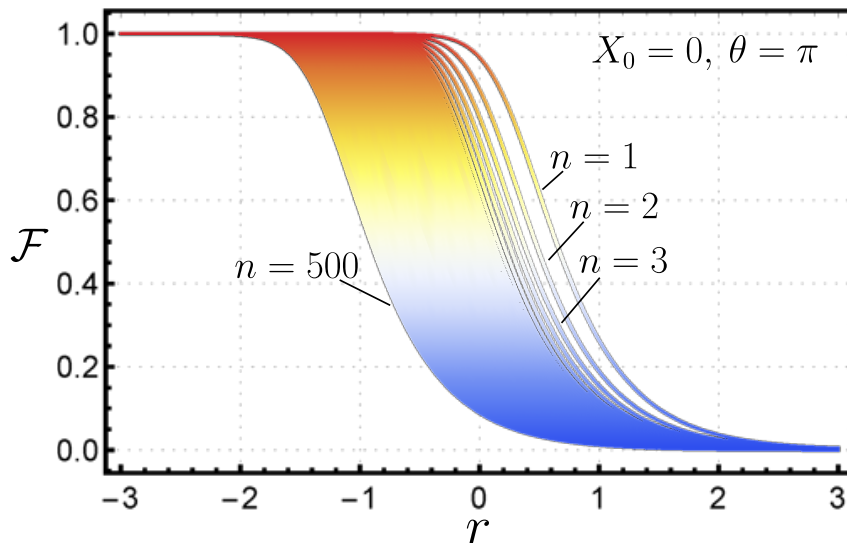


Figure 8: Curves for the fidelity of teleportation ($X_0 = 0$, $\theta = \pi$) of a squeezed-coherent state for a chain of $n = 1 - 500$ successive clusters. As the number of clusters in the chain increases, the peaks of the curves displace towards the region $r < 0$, which means that a higher degree of squeezing in momentum for each squeezed vacuum state is required to reach high-quality teleportation ($\mathcal{F} \approx 1$).

To show the behavior of the fidelity of teleportation of the squeezed-coherent state in sequential clusters, we consider that all squeezed vacuum states of the chain have the same wave function: $f_{G(i)}(q) = f_G(q)$, as is given by Eq. (3.11); besides, we assume that the squeezed-coherent state under teleportation has the same squeezing than all squeezed vacuum states of the chain; therefore we have $r_1 = r_2 = r$ and $\delta_{q_i}^2 = \delta_q^2(r, \theta) = e^{-2r}$. With these considerations, in Fig. 7, we show the plots describing the behavior of the fidelity of teleportation of a squeezed-coherent through $n = 1, 15$, and 200 successive clusters. From these plots, we can conclude that as the squeezed-coherent state is teleported across a larger chain, the fidelity of teleportation will reduce; this effect comes from the accumulated Gaussian distortions that arise from each teleportation event in the chain; however, as we explain in Subsection 3.4, such noise can be lessened through the handling of the effective displacement X_0 ; that is, it is possible to engineer a configuration where the squeezed-coherent state has an adequate localization in the phase space and then select appropriate selectivity

intervals for the measurements in each cluster such that the net effective displacement converges to a value proximate to zero, where we will obtain the maximum fidelities of teleportation.

On the other hand, as is verified from (a) and (b) of Fig. 7, the maximums in the fidelity happen at the region of momentum squeezing ($r < 0$): then, by considering the case of $X_0 = 0$, we carry out a numerical maximization to explore the rotation angle θ at which exist the peaks for the fidelity inside $r < 0$ for $n = 1 - 500$; in all cases, we find $\theta \approx \pi$. Notably, even with these appropriate parameters, we will need increase more and more the squeezing in momentum of the squeezed vacuum states of the chain to support high-quality teleportation over progressively longer chains; see Fig. 8. Therefore, we verify again a complementary behavior between the probability and the fidelity of teleportation, where the quality of the former is linked with the squeezing in position, while the second is with the squeezing in momentum.

5 Conclusions

The present work uncovers key features concerned with the building block of one-way quantum computation with continuous variables; that is, the teleportation process with a two-mode continuous variable cluster state.

We take the fact that projective measurements in the continuous-variable regime can not be infinitely selective; there exists an infinite of possible measurement outputs that are probabilistically distributed on an interval called the selectivity interval of the measurement apparatus, which essentially constitutes its range of detection. By employing this concept in the teleportation through a two-mode continuous-variable cluster state, we derive the mathematical expression governing the probability of teleportation, as the formalism of the quantum measurement demands it. Particularly, we find that the probability of teleportation constitutes the mirror image of the generalized Weierstrass transform of the position probability distribution associated with the system under teleportation; notably, this expression constitutes a valid solution of the heat equation.

On the other hand, by considering the quasi-selective approximation in the insufficiently selective measurement, we get the expression that describes the fidelity of teleportation in the cluster; remarkably, we show that such expression constitutes a quotient between the squared solution of a non-homogeneous heat equation and that of the traditional heat equation. Remarkably, we find that both the fidelity and the probability of teleportation of a single cluster present a complementary behavior regarding the selectivity interval of the measurement and the squeezing of the squeezed vacuum state; that is, by decreasing the width of the selectivity interval we diminish the probability of teleportation but the fidelity increase, and vice versa. Besides, the likelihood of teleportation increases with the increase of the squeezing in position of the squeezed vacuum state while the fidelity rises with the growth of the squeezing in momentum.

Notably, both the probability and the fidelity of teleportation are directly dependent on the overlap (formally, the convolution) between the wave functions of the squeezed vacuum and the teleported state building the cluster; such overlap depends on the squeezing of the states, but also on the possible measurement outcomes attainable in the cluster; then, this fact situate the formalism of an insufficiently selective measurement apparatus as an adequate medium to handle the Gaussian noise affecting the quality of teleportation in a two-mode continuous variable cluster state.

On the other hand, we consider a linear scheme of sequential teleportations with intermediate corrections. Particularly, we obtain the exact expression governing the probability of teleportation in the sequence; it depends on the preparation of each squeezed vacuum state and each measurement result at each step of the chain. In addition, we determine that the fidelity of teleportation in this recursive model also depends on each of the Gaussian wave functions of the individual squeezed vacuum states building the chain; then, each teleportation process add a Gaussian envelope that affects the quality of the whole fidelity. Besides, we find that the fidelity of teleportation maintains the same mathematical shape as in the case of teleportation through a single cluster; this means that our linear teleportation scheme is indistinct of a teleportation process involving one single cluster.

We find that both the probability and the fidelity of teleportation in a linear cluster also depend on the overlap between the resultant Gaussian function of the chain and the position probability

distribution of the quantum state under teleportation; then, this fact also situates the bounding of the measurement results due to insufficiently selective measurements as an important mechanism to select those outcomes that allow handling both the probability and the fidelity of teleportation in the scheme of successive teleportations.

We have found a complementary behavior between the probability and fidelity of teleportation in the linear sequence of clusters. Specifically, we observe that as the number of clusters in the chain increases, the fidelity decreases while the probability of successful teleportation increases, and vice versa. Besides, as in the case of one single cluster, the probability of teleportation increases with the growth of the squeezing in position of the squeezed vacuum states of the chain, while the fidelity is higher with the increase of the squeezing in momentum.

Finally, the present work provides the mathematical expressions to describe the quality of teleportation—probability and fidelity—in sequential teleportations, which serves as a medium to design and engineer efficient teleportation linear schemes through two-mode continuous variable cluster states.

Acknowledgements

J. A. Mendoza-Fierro thanks CONAHCYT for the postdoctoral fellowship support under the application number 3762623.

References

- [1] Michael A Nielsen and Isaac L Chuang. Quantum computation and quantum information. *Phys. Today*, 54(2):60, 2001.
- [2] Yan Wang, Jungin E Kim, and Krishnan Suresh. Opportunities and challenges of quantum computing for engineering optimization. *Journal of Computing and Information Science in Engineering*, 23(6):060817, 2023.
- [3] Akshay Ajagekar, Travis Humble, and Fengqi You. Quantum computing based hybrid solution strategies for large-scale discrete-continuous optimization problems. *Computers & Chemical Engineering*, 132:106630, 2020.
- [4] Andrew J Daley, Immanuel Bloch, Christian Kokail, Stuart Flannigan, Natalie Pearson, Matthias Troyer, and Peter Zoller. Practical quantum advantage in quantum simulation. *Nature*, 607(7920):667–676, 2022.
- [5] Iulia M Georgescu, Sahel Ashhab, and Franco Nori. Quantum simulation. *Reviews of Modern Physics*, 86(1):153, 2014.
- [6] Peter W Shor. Polynomial-time algorithms for prime factorization and discrete logarithms on a quantum computer. *SIAM review*, 41(2):303–332, 1999.
- [7] Ivan H Deutsch. Harnessing the power of the second quantum revolution. *PRX Quantum*, 1(2):020101, 2020.
- [8] Dong-Sheng Wang. A comparative study of universal quantum computing models: Toward a physical unification. *Quantum Engineering*, 3(4):e85, 2021.
- [9] Maarten Van den Nest, Wolfgang Dür, Akimasa Miyake, and Hans J Briegel. Fundamentals of universality in one-way quantum computation. *New Journal of Physics*, 9(6):204, 2007.
- [10] Robert Raussendorf and Hans J Briegel. A one-way quantum computer. *Physical review letters*, 86(22):5188, 2001.
- [11] Dan Browne and Hans Briegel. One-way quantum computation. *Quantum information: From foundations to quantum technology applications*, pages 449–473, 2016.

- [12] David Gross, Jens Eisert, Norbert Schuch, and David Perez-Garcia. Measurement-based quantum computation beyond the one-way model. *Physical Review A*, 76(5):052315, 2007.
- [13] Robert Raussendorf, Jim Harrington, and Kovid Goyal. A fault-tolerant one-way quantum computer. *Annals of physics*, 321(9):2242–2270, 2006.
- [14] Nicolas C Menicucci. Fault-tolerant measurement-based quantum computing with continuous-variable cluster states. *Physical review letters*, 112(12):120504, 2014.
- [15] Keisuke Fujii and Yuuki Tokunaga. Fault-tolerant topological one-way quantum computation with probabilistic two-qubit gates. *Physical review letters*, 105(25):250503, 2010.
- [16] Daniel Gottesman, Alexei Kitaev, and John Preskill. Encoding a qubit in an oscillator. *Physical Review A*, 64(1):012310, 2001.
- [17] Philip Walther, Kevin J Resch, Terry Rudolph, Emmanuel Schenck, Harald Weinfurter, Vlatko Vedral, Markus Aspelmeyer, and Anton Zeilinger. Experimental one-way quantum computing. *Nature*, 434(7030):169–176, 2005.
- [18] Seth Lloyd and Samuel L Braunstein. Quantum computation over continuous variables. *Physical Review Letters*, 82(8):1784, 1999.
- [19] Jing Zhang and Samuel L Braunstein. Continuous-variable gaussian analog of cluster states. *Physical Review A*, 73(3):032318, 2006.
- [20] Nicolas C. Menicucci, Peter van Loock, Mile Gu, Christian Weedbrook, Timothy C. Ralph, and Michael A. Nielsen. Universal quantum computation with continuous-variable cluster states. *Phys. Rev. Lett.*, 97:110501, Sep 2006.
- [21] Xinlan Zhou, Debbie W Leung, and Isaac L Chuang. Methodology for quantum logic gate construction. *Physical Review A*, 62(5):052316, 2000.
- [22] Michael A Nielsen. Cluster-state quantum computation. *Reports on Mathematical Physics*, 57(1):147–161, 2006.
- [23] Daiqin Su, Christian Weedbrook, and Kamil Brádler. Correcting finite squeezing errors in continuous-variable cluster states. *Physical Review A*, 98(4):042304, 2018.
- [24] Shuhong Hao, Xiaowei Deng, Yang Liu, Xiaolong Su, Changde Xie, and Kunchi Peng. Quantum computation and error correction based on continuous variable cluster states. *Chinese Physics B*, 30(6):060312, 2021.
- [25] Kosuke Fukui, Akihisa Tomita, Atsushi Okamoto, and Keisuke Fujii. High-threshold fault-tolerant quantum computation with analog quantum error correction. *Physical review X*, 8(2):021054, 2018.
- [26] Kyungjoo Noh and Christopher Chamberland. Fault-tolerant bosonic quantum error correction with the surface–gottesman-kitaev-preskill code. *Physical Review A*, 101(1):012316, 2020.
- [27] Mikkel V Larsen, Jonas S Neergaard-Nielsen, and Ulrik L Andersen. Architecture and noise analysis of continuous-variable quantum gates using two-dimensional cluster states. *Physical Review A*, 102(4):042608, 2020.
- [28] Mikkel V Larsen, Christopher Chamberland, Kyungjoo Noh, Jonas S Neergaard-Nielsen, and Ulrik L Andersen. Fault-tolerant continuous-variable measurement-based quantum computation architecture. *Prx Quantum*, 2(3):030325, 2021.
- [29] J Eli Bourassa, Rafael N Alexander, Michael Vasmer, Ashlesha Patil, Ilan Tzitrin, Takaya Matsuura, Daiqin Su, Ben Q Baragiola, Saikat Guha, Guillaume Dauphinais, et al. Blueprint for a scalable photonic fault-tolerant quantum computer. *Quantum*, 5:392, 2021.

- [30] Ilan Tzitrin, Takaya Matsuura, Rafael Alexander, Guillaume Dauphinais, J Eli Bourassa, Krishna Sabapathy, Nicolas Menicucci, and Ish Dhand. Fault-tolerant quantum computation with static linear optics, prx quantum. *Physics Review Journal*, 2021.
- [31] Kyungjoo Noh, Christopher Chamberland, and Fernando GSL Brandão. Low-overhead fault-tolerant quantum error correction with the surface-gkp code. *PRX Quantum*, 3(1):010315, 2022.
- [32] SB Korolev and T Yu Golubeva. Error correction of the continuous-variable quantum hybrid computation on two-node cluster states: Limit of squeezing. *Physics Letters A*, 441:128149, 2022.
- [33] Kosuke Fukui. High-threshold fault-tolerant quantum computation with the Gottesman-Kitaev-Preskill qubit under noise in an optical setup. *Physical Review A*, 107(5):052414, 2023.
- [34] Peilin Du, Jing Zhang, Tiancai Zhang, Rongguo Yang, and Jiangrui Gao. A complete continuous-variable quantum computation architecture: from cluster state generation to fault-tolerant accomplishment. *arXiv preprint arXiv:2312.13877*, 2023.
- [35] ER Zinatullin, SB Korolev, AD Manukhova, and T Yu Golubeva. Error of an arbitrary single-mode gaussian transformation on a weighted cluster state using a cubic phase gate. *Physical Review A*, 106(3):032414, 2022.
- [36] ER Zinatullin, SB Korolev, and T Yu Golubeva. Controlled-z operation versus the beam-splitter transformation: Errors of entangled operations. *Physical Review A*, 103(6):062407, 2021.
- [37] Mile Gu, Christian Weedbrook, Nicolas C Menicucci, Timothy C Ralph, and Peter van Loock. Quantum computing with continuous-variable clusters. *Physical Review A*, 79(6):062318, 2009.
- [38] Claude Cohen-Tannoudji, Bernard Diu, and Franck Lalœ. *Quantum mechanics*. John Wiley & Sons, New York, 1977.
- [39] Arun K Pati, Samuel L Braunstein, and Seth Lloyd. Quantum searching with continuous variables. *arXiv preprint quant-ph/0002082*, 2000.
- [40] Christian Weedbrook, Stefano Pirandola, Raúl García-Patrón, Nicolas J Cerf, Timothy C Ralph, Jeffrey H Shapiro, and Seth Lloyd. *Rev. Mod. Phys.*, 84(2):621, 2012.
- [41] Matteo GA Paris. The modern tools of quantum mechanics: A tutorial on quantum states, measurements, and operations. *The European Physical Journal Special Topics*, 203(1):61–86, 2012.
- [42] Nicolas C. Menicucci, Xian Ma, and Timothy C. Ralph. Arbitrarily large continuous-variable cluster states from a single quantum nondemolition gate. *Phys. Rev. Lett.*, 104:250503, Jun 2010.
- [43] Andrew N Jordan and Irfan A Siddiqi. *Quantum Measurement: Theory and Practice*. Cambridge University Press, 2024.
- [44] Pieter Kok and Brendon Lovett W. *Introduction to quantum information processing*. Cambridge University Press, New York, 2010.
- [45] Daniel F Walls and Gerard J Milburn. *Quantum optics*. Springer Springer, Berlin, 1994.
- [46] Akira Furusawa. Hybrid quantum information processing. *AIP Conference Proceedings*, 1633(1):100–105, 2014.
- [47] Olivier Pfister. Continuous-variable quantum computing in the quantum optical frequency comb. *Journal of Physics B: Atomic, Molecular and Optical Physics*, 53(1):012001, 2019.

- [48] Ryuji Ukai. Experimental demonstration of controlled-z gate for continuous variables. In *Multi-Step Multi-Input One-Way Quantum Information Processing with Spatial and Temporal Modes of Light*, pages 197–231. Springer, 2014.
- [49] Samuel L Braunstein. Squeezing as an irreducible resource. *Physical Review A—Atomic, Molecular, and Optical Physics*, 71(5):055801, 2005.
- [50] B Yurke. Optical back-action-evading amplifiers. *JOSA B*, 2(5):732–738, 1985.
- [51] Ming-Feng Wang, Nian-Quan Jiang, Qing-Li Jin, and Yi-Zhuang Zheng. Continuous-variable controlled-z gate using an atomic ensemble. *Phys. Rev. A*, 83:062339, Jun 2011.
- [52] Jun-ichi Yoshikawa, Yoshichika Miwa, Alexander Huck, Ulrik L Andersen, Peter van Loock, and Akira Furusawa. Demonstration of a quantum nondemolition sum gate. *Physical Review Letters*, 101(25):250501, 2008.
- [53] John Neumann, Eugene Paul Wigner, and Robert Hofstadter. *Mathematical foundations of quantum mechanics*. Princeton university press, 1955.
- [54] Sergey V Polyakov. Photomultiplier tubes. In *Experimental Methods in the Physical Sciences*, volume 45, pages 69–82. Elsevier, 2013.
- [55] Mohammed Ismail and Mohamad Sawan. Analog circuits and signal processing. 2013.
- [56] Ling-An Wu, HJ Kimble, JL Hall, and Huifa Wu. Generation of squeezed states by parametric down conversion. *Physical review letters*, 57(20):2520, 1986.
- [57] A. I. Lvovsky. *Squeezed Light*, chapter 5, pages 121–163. John Wiley & Sons, Ltd, 2015.
- [58] Scott M. Cohen. Local distinguishability with preservation of entanglement. *Phys. Rev. A*, 75:052313, May 2007.
- [59] Ahmed I Zayed. *Handbook of function and generalized function transformations*. CRC press, 1996.
- [60] Samuel L Braunstein, Christopher A Fuchs, and HJ Kimble. Criteria for continuous-variable quantum teleportation. *Journal of Modern Optics*, 47(2):267–278, 2000.
- [61] Eduardo Munguia-Gonzalez, Sheldon Rego, and JK Freericks. Making squeezed-coherent states concrete by determining their wavefunction. *American Journal of Physics*, 89(9):885–896, 2021.
- [62] MOSM Hillery, Robert F O’Connell, Marlan O Scully, and Eugene P Wigner. Distribution functions in physics: Fundamentals. *Physics reports*, 106(3):121–167, 1984.
- [63] William B Case. Wigner functions and weyl transforms for pedestrians. *American Journal of Physics*, 76(10):937–946, 2008.
- [64] Henning Vahlbruch, Moritz Mehmet, Karsten Danzmann, and Roman Schnabel. Detection of 15 db squeezed states of light and their application for the absolute calibration of photoelectric quantum efficiency. *Phys. Rev. Lett.*, 117:110801, Sep 2016.
- [65] H-J Briegel, Wolfgang Dür, Juan I Cirac, and Peter Zoller. Quantum repeaters: the role of imperfect local operations in quantum communication. *Physical Review Letters*, 81(26):5932, 1998.
- [66] Paul Bromiley. Products and convolutions of gaussian probability density functions. *Tina-Vision Memo*, 3(4):1, 2003.
- [67] Gerd Niestegge. An approach to quantum mechanics via conditional probabilities. *Foundations of Physics*, 38(3):241–256, 2008.